12-2009

Physical and Functional Coupling of CFTR and PDE3A

Himabindu Penmatsa
University of Tennessee Health Science Center

Physical and Functional Coupling of CFTR and PDE3A

DOI
10.21007/etd.cghs.2009.0240

PHYSICAL AND FUNCTIONAL COUPLING OF CFTR AND PDE3A

A Dissertation
Presented for
The Graduate Studies Council
The University of Tennessee
Health Science Center

In Partial Fulfillment
Of the Requirements for the Degree
Doctor of Philosophy
From The University of Tennessee

By
Himabindu Penmatsa
December 2009

DEDICATION

This dissertation is dedicated to my parents, Rajeswari Penmatsa and Dattatreyavarma Penmatsa for being my strength, for their unconditional love, and constant support and to Dr. A. P. Naren for providing me this amazing opportunity.

ACKNOWLEDGEMENTS

I am grateful to my mentor Dr. A. P. Naren for continued support and motivation all through my research training. His positive attitude towards research, knowledge and endurance has made my research journey very fruitful and enjoyable. I am also thankful to my former advisor Dr. G. N. Sastry for helping me realize my passion for research.

I am thankful to my committee members Drs. Ioannis Dragatsis, Ivan Gerling, Donald Thomason, and Xin Zhang for their valuable suggestions and guidance.

I would like to thank my lab members Li, Weiqiang, Sunitha, Aixia, and Veronica for technical assistance, help and support.

I would like to thank Drs. Deborah Nelson and Guangping Zhang for technical assistance with single-channel recording experiments. I would like to thank Drs. Jeffrey Wine and Monal Sonecha for teaching me submucosal gland secretion assay. I would like to thank Drs. Suleiman Bahouth and Junming Yue for assistance with cloning. I thank Shirley Hancock, Patricia Page, and Larry Tague for assistance with dissertation preparation.

I would like to thank and appreciate the grant support from American Heart Association and J. Paul Quigley award.

I express my sincere gratitude to my mom and dad for their unconditional love and support and to my brother and sister-in-law for always being there in times of need.

I truly appreciate the encouragement and immense moral support of my friends Sunitha, Deepthi, Vasanthi, Bharathi, and Surekha in times good and bad.

ABSTRACT

Formation of multiple-protein macromolecular complexes at specialized subcellular microdomains increases the specificity and efficiency of signaling in cells. In this study, we demonstrated that phosphodiesterase type 3A (PDE3A) is physically and functionally coupled to cystic fibrosis transmembrane conductance regulator (CFTR). PDE3A inhibition increases cyclic adenosine 3′, 5′-monophosphate (cAMP) levels in a compartmentalized manner at the plasma membrane, which potentiates CFTR channel function and further clusters PDE3A and CFTR into microdomains. Actin skeleton disruption reduces PDE3A-CFTR interaction and segregates PDE3A from its interacting partners, thus compromising the integrity of the macromolecular complex. Consequently, PDE3A inhibition no longer activates CFTR channel function in a compartmentalized manner. Physiologically, formation of the CFTR-PDE3A-containing macromolecular complexes was investigated using pig trachea submucosal gland secretion model. PDE3A inhibition augments CFTR-dependent submucosal gland secretion and actin skeleton disruption decreases secretion. These findings are important in understanding the regulation of CFTR function by phosphodiesterases.

TABLE OF CONTENTS

LIST OF FIGURES

LIST OF ABBREVIATIONS

β_2-AR	β_2-adrenergic receptor
μ	micro
AC	adenylyl cyclase
AKAP	A-kinase-anchoring protein
AMP	adenosine monophosphate
ANOVA	analysis of variance
AR	adrenergic receptor
ATP	adenosine triphosphate
BIG	brefeldin-A inhibited guanine nucleotide exchange protein
BSA	bovine serum albumin
C	carboxyl end
Ca^{2+}	calcium
CAL	CFTR associated ligand
Calu-3	human, Caucasian, lung, adenocarcinoma
CaM	calcium modulated protein
cAMP	adenosine-3', 5'-cyclicmonophosphate
CAP70	cftr-associated protein-70kDa
cDNA	complementary DNA
CF	cystic fibrosis
CFP	cyan fluorescent protein
CFTR	cystic fibrosis transmembrane conductance regulator
cGMP	guanosine-3', 5'-cyclicmonophosphate

COPD	chronic obstructive pulmonary disease
cpt.cAMP	8-(4-chlorophenylthio) adenosine-3', 5'-cyclicmonophosphate
D	diffusion coefficient
DMEM-F12	Dulbecco's modified eagle medium with nutrient mixture F-12
DSP	dithiobis (succinimidyl) propionate
DTT	dithiothreitol
EDTA	ethylene diamine tetraacetic acid
EM-CCD	electron multiplying charge coupled device
EPAC	exchange protein directly activated by cAMP
FRET	fluorescence resonance energy transfer
G418	genetecin
GPCR	G-protein coupled receptor
GST	glutathione-S-transferase
^{3}H	tritium
HA	hemagglutinin
HBSS	Hank's buffered salt solution
HCl	hydrochloric acid
HEK-293	human embryonic kidney-293
Hepes	4-(2-hydroxyethyl)-1-piperazineethanesulfonic acid
HIS	histidine
HRP	horse-radish peroxidase
H_2SO_4	sulphuric acid
IBMX	3-isobutyl-1-methylxanthine

IgG	immunoglobulin G
IκB	IkappaB protein
Inh	inhibitor
IP	immuno-precipitation
IPTG	isopropyl-β-D-1 thiogalactopyranoside
I_{SC}	short-circuit current
KCl	potassium chloride
K_2HPO_4	dipotassium hydrogen phosphate
KH_2PO_4	monopotassium hydrogen phosphate
LIC	ligation independent cloning
LPA_2	lysophosphatidic acid receptor-2
M	Molar
mAb	monoclonal antibody
mAKAP	muscle AKAP
ME	mercaptoethanol
MEM	minimal essential medium
mg	milligram
$MgCl_2$	magnesium chloride
min	minute
ml	milliliter
mm	millimeter
mM	millimolar
MRP4	multidrug resistance protein 4

MSD	mean squared displacement
mV	millivolts
N	amino terminal end
Na^+	sodium
NaCl	sodium chloride
$NaHCO_3$	sodium bicarbonate
NaI	sodium iodide
$NaNO_3$	sodium nitrate
NBD	nucleotide binding domain
N-FRETc	normalized corrected FRET
ng	nanograms
NHERF	Na+/H+ exchange regulatory factor
nl	nanoliter
nM	nanomolar
P	probability
PAGE	polyacrylamide gel electrophoresis
PDE	phosphodiesterase
PDZ	PSD95/DlgA/zo-1
PKA	protein kinase A
PMSF	phenyl methyl sulfonyl fluoride
PSD95	post synaptic density protein
PVDF	polyvinylidene difluoride
RIPA	radioimmunoprecipitation

SD	standard deviation
SDS	sodium dodecyl sulfate
SEM	standard error of the mean
SNAP-23	soluble NSF attachment protein of 23 kilodaltons
SPT	single particle tracking
TBS	Tris-base saline
TMB	tetramethyl benzidine
VIP	vasoactive intestinal peptide
wt	wild-type
YFP	yellow fluorescent protein
ZO-1	zonula occludens-1 protein

CHAPTER 1: INTRODUCTION

Phosphodiesterases

Cyclic nucleotides and signaling

Cyclic adenosine-3′,5′-monophosphate (cAMP) and cyclic guanosine-3′,5′-monophosphate (cGMP) are important secondary messengers in the cells. Their levels have to be maintained precisely to regulate a variety of signaling cascades and cellular processes such as metabolism, cell proliferation and differentiation, secretion, vascular and airway smooth muscle relaxation and production of inflammatory mediators (Thompson et al., 2007; Zaccolo, 2006). cAMP effects are through activation of a limited number of effectors including cAMP-dependent protein kinase A (PKA), GTP-exchange protein EPACs (exchange proteins activated by cAMP) and via cAMP-gated ion channel (Halpin, 2008; Thompson et al., 2007). There is accumulating evidence for subcellular compartmentalization of cAMP, permitting control of cAMP-dependent signal transduction both spatially and temporally (Cooper, 2005; Halpin, 2008; Li et al., 2007).

Cyclic nucleotide phosphodiesterases

Cyclic nucleotide phosphodiesterases (PDEs) catalyze the hydrolysis of the 3′,5′-phosphodiester bond of cyclic nucleotides and thus play pivotal roles in regulating intracellular concentrations and effects of secondary messengers cAMP and cGMP (Beavo, 1995; Degerman et al., 1997). PDEs have been reported to interact with regulatory proteins, scaffolding proteins and other signaling molecules to form macromolecular complexes which increase specificity and efficiency in cAMP signaling (Conti & Beavo, 2007). Eleven families of mammalian PDEs (PDE1-11) have been reported. Most of the families have more than one member. PDE3 family has two isoforms, PDE3A and PDE3B. PDE3s have distinctive characteristics which distinguish them from other PDEs, e.g., an insert of 44 amino acids in the catalytic domain and six hydrophobic putative transmembrane domains at the N-terminus. The structural organization of PDE3A and PDE3B protein is identical. However, the two isoforms exhibit tissue-specific expression and distinct cellular distributions (Conti & Beavo, 2007; Degerman et al., 1997; Meacci et al., 1992). PDE3s have high affinities for both cAMP and cGMP (K_m between 0.1-0.8μM) with V_{max} for cAMP much higher than for cGMP (Beavo, 1995; Conti et al., 1995; Degerman et al., 1997; Manganiello et al., 1995). PDE3 is also called cGMP-inhibited PDE because of its inhibition by cGMP (Beavo, 1995; Conti et al., 1995; Manganiello et al., 1995). PDE3A has been shown to be phosphorylated and activated by PKA, PKB and PKC in smooth muscle, oocytes and platelets respectively (Han et al., 2006; Hunter et al., 2009; Murthy et al., 2002).

Phosphodiesterase 3

PDE3A is the major isoform expressed in the heart, lung, and platelets where it regulates physiological processes such as contraction of heart, relaxation of bronchial smooth muscle, and platelet aggregation (Shakur et al., 2001). A pictorial representation of PDE3A protein structure is shown in Fig. 1-1. PDE3B is highly expressed in hepatocytes, adipocytes and beta cells and has been identified as a potential target for the treatment of obesity and diabetes (Thompson et al., 2007). Specific PDE3 inhibitors, presumably by inhibiting PDE3A, have been reported to enhance myocardial contractility and induce vascular and airway smooth muscle relaxation and have been used to treat heart failure and intermittent claudication (Halpin, 2008; Liu et al., 2001; Shin et al., 2007). PDE inhibitors have also been shown to activate CFTR function in airway and colonic epithelial cells (Kelley et al., 1995; Liu et al., 2005).

Cystic Fibrosis Transmembrane Conductance Regulator

CFTR in fluid homeostasis and regulation

CFTR is a cAMP-regulated chloride channel localized primarily at the apical surfaces of epithelial cells lining airway, gut, exocrine glands, etc., where it is responsible for transepithelial salt and water transport (Anderson et al., 1991; Bear et al., 1992; Riordan et al., 1989). CFTR function is also critical in maintaining fluid homeostasis, airway fluid clearance, and tracheal mucosal secretion in healthy and disease phenotypes (Riordan, 2008; Wine & Joo, 2004). CFTR is regulated by the activities of adenylyl cyclase (ACs) and PDEs through cAMP (Liu et al., 2005). A growing number of studies suggest that CFTR interacts directly or indirectly with other transporters, ion channels, scaffolding proteins, protein kinase, and cytoskeletal elements to form macromolecular complexes (Li et al., 2005; Li & Naren, 2005; Naren et al., 2003; Yoo et al., 2004).

CFTR and mutations

The CFTR gene encodes a 1480 amino acid chloride channel protein with twelve putative transmembrane domains (TMDs), two nucleotide binding domains (NBDs) and a regulatory (R) domain (Riordan, 2005). A pictorial representation of CFTR protein is shown in Fig. 1-2. Mutations in CFTR gene cause the expression of abnormal or non-functional chloride channel in most cases thereby causing the disease cystic fibrosis (CF). Cystic fibrosis is a lethal autosomal recessive disorder usually associated with lung disease, pancreatic insufficiency, and elevated sweat chloride levels (Quinton, 1986; Rowntree & Harris, 2003). Although there are more than 1500 mutations described for the CFTR gene, mutations in CF patients can be divided into six classes (Amaral & Kunzelmann, 2007; Benharouga et al., 2001; Haardt et al., 1999; Rowntree & Harris, 2003; Zielenski & Tsui, 1995; Zielenski, 2000). The class I mutations constitute

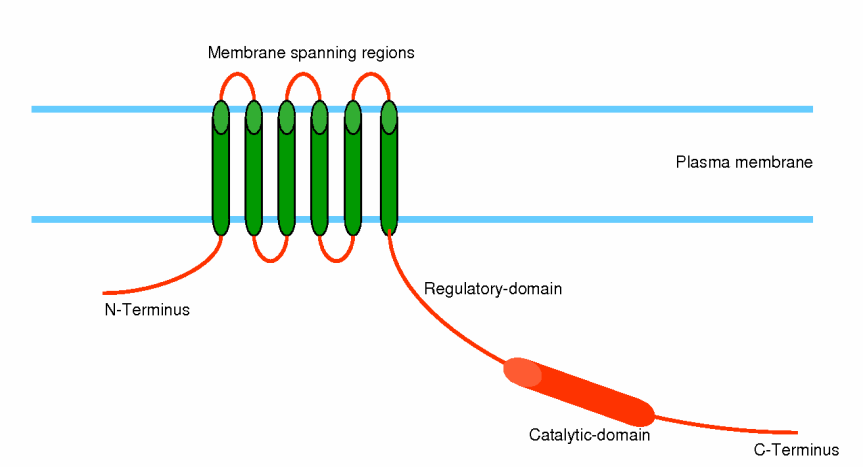

Figure 1-1. Pictorial representation of PDE3A

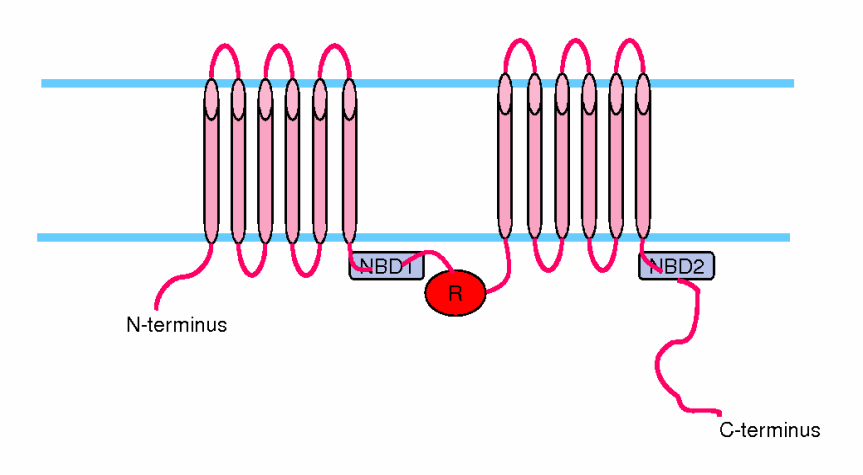

Figure 1-2. Pictorial representation of CFTR showing transmembrane domains, nucleotide binding (NBDs) domains, and regulatory (R) domain

nonsense, splice and frame shift mutants that encode truncated forms of CFTR. The class II mutations are mostly processing mutants that get trapped in the endoplasmic reticulum (ER). The class III are regulation mutants and class IV are permeation mutants with partial loss of function. The class V mutations show reduced mRNA stability. The class VI mutations include C-terminal truncated CFTR which forms unstable mature protein with several fold faster degradation rate than WT-CFTR.

Actin cytoskeleton and CFTR

The role of actin filaments in regulating the function and organization of ion channels has been long established (Cantiello et al., 1991; Cantiello et al., 1993; Cantiello, 1996). Actin cytoskeleton disruption has been shown to affect both CFTR currents and the diffusion of the protein at the membrane (Cantiello, 2001; Ganeshan et al., 2007; Haggie et al., 2006). Actin depolymerizing reagent latrunculin B was shown to cause changes in CFTR dynamics (Haggie et al., 2006). Also, evidence for a direct interaction between purified CFTR and actin has been provided by reconstituting CFTR in lipid bilayer (Chasan et al., 2002). Given the evidence, it is logical to predict that actin cytoskeleton plays an important role in maintaining the integrity of CFTR protein-protein interactions as well.

Protein-protein Interactions and Compartmentalized cAMP Signaling

CFTR protein-protein interactions

The physical and functional coupling of multiple proteins involved in a complex in compartmentalized domains is logical to achieve specific local signaling responses. The role of macromolecular complex formation in compartmentalized signaling has been elucidated for CFTR (Li & Naren, 2005; Li et al., 2007). The predominant adrenergic receptor isoform in the airway epithelia is β_2-adrenergic receptor (Abraham et al., 2003). In airway epithelial cells, it has been shown that β_2AR agonists activate CFTR function (Li & Naren, 2005). Also CFTR was shown to form macromolecular complexes with receptors and scaffolding proteins (LPA_2, β_2AR, NHERFs) to form a spatially, and temporally, regulated localized cAMP signaling complex (Li et al., 2005; Li et al., 2007; Naren et al., 2003). The role of PKA in regulating the function of CFTR in these signaling complexes has been proved as well (Naren et al., 2003). Earlier, syntaxin 1A and SNAP-23 were shown to bind CFTR and downregulate its activity (Naren et al., 1997; Naren et al., 1998; Peters et al., 1999). Several PDZ proteins were shown to bind CFTR which include NHERF1, NHERF2, CAP70, CAL and IKEPP (Cheng et al., 2002; Hall et al., 1998; Short et al., 1998; Sun et al., 2000; Wang et al., 2000). Recently, it has been shown that CFTR couples to MRP4 via CAP70 scaffolding protein to form a temporally and spatially isolated microdomain for cAMP regulation of CFTR function (Li et al., 2007). Such protein-protein interactions have been shown to play key roles in pathophysiology as well. Altering CFTR function via its coupling to MRP4 or LPA_2 has

been shown to inhibit secretory diarrhea in mice in vivo (Li et al., 2005; Li et al., 2007). A schematic of plausible CFTR macromolecular complex is shown in Fig. 1-3.

PDE protein-protein interactions

Phosphodiesterases such as PDE1, PDE3, PDE4, PDE6, PDE7 & PDE8 have been shown to form higher order complexes and to be involved in protein-protein interactions that regulate their function (Conti & Beavo, 2007). Interactions like CaM with PDE1 and Xap2 with PDE4A5 are a few examples to implicate the importance of protein-protein interactions in regulation of PDE activity (Bolger et al., 2003; Florio et al., 1996). Shank 2 has been shown to interact with PDE4D and bring it physically close to CFTR (Lee et al., 2007). PDEs have also been shown to interact with scaffolding proteins like AKAPs bringing protein kinases into the macromolecular complex (Dodge-Kafka et al., 2006). For example, mAKAP and AKAP 450 have been shown to bind PDE4D3 and form a complex, which can be tightly regulated by PKA in micro-domains (Dodge et al., 2001; Tasken et al., 2001). PKA in this complex has been shown to increase protein-protein interactions of PDE in the complex, and alter cAMP levels locally by activating PDE. PDE4 has also been shown to interact with arrestin and this interaction has been suggested to play an important role in receptor signaling (Perry et al., 2002). PDE3 interaction with 14-3-3 and PDE 8 interaction with IκB are examples of other PDE protein-protein interactions (Onuma et al., 2002; Wu & Wang, 2004). The importance of these macromolecular complexes at a physiological level has been shown in PDE4D null mice, in which, the dysfunction of the complex has been implicated to play a role in progression of cardiac failure and arrhythmias seen under stress in these mice (Lehnart et al., 2005). The existence of PDEs as dimers or oligomers in the cell has also been reported for several isoforms (Conti & Beavo, 2007). There is a speculation that loss of oligomerization leads to loss of catalytic activity, also, a change in affinity of catalytic domain to certain inhibitors has been observed (Conti & Beavo, 2007; Richter & Conti, 2004).

CFTR and Tracheal Submucosal Gland Secretion

Submucosal gland structure and function

Submucosal glands in the trachea secrete several substances including mucins, anti-microbial substances and fluid which primarily form the mucus as a protective line of defense. These glands contain ducts and secretory tubules (Meyrick et al., 1969). The secretory tubules contain serosal and mucosal cells. A pictorial representation of submucosal gland structure is shown in Fig. 1-4. Mucous cells secrete mucins and serous cells secrete fluid and anti-microbial substances thereby providing a medium of protection (Basbaum et al., 1990; Meyrick & Reid, 1970). CFTR protein expression is found predominantly in the serosal cells of the submucosal glands and also in the apical plasma membrane of ciliated cells (Engelhardt et al., 1992; Jacquot et al., 1993). CFTR is

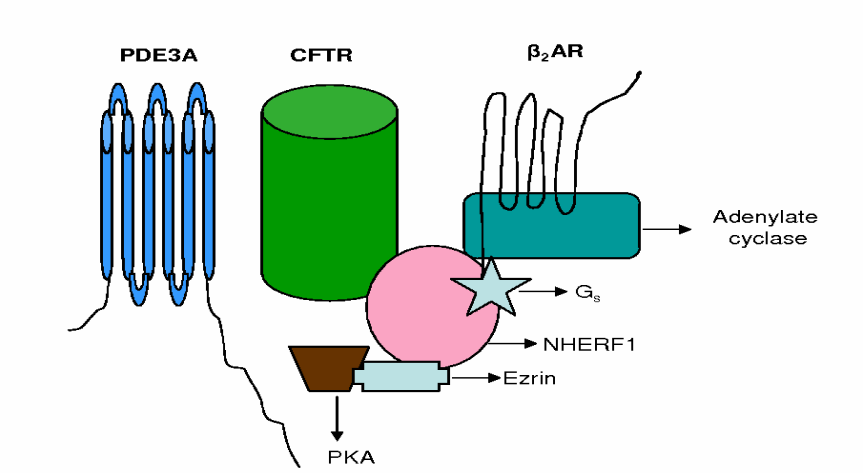

Figure 1-3. CFTR macromolecular complex. Modified from source: Naren, A.P., Cobb, B., Li, C., Roy, K., Nelson, D., Heda, G.D., Liao, J., Kirk, K.L., Sorscher, E.J., Hanrahan, J. & Clancy, J.P. (2003). A macromolecular complex of beta 2 adrenergic receptor, CFTR, and ezrin/radixin/moesin-binding phosphoprotein 50 is regulated by PKA. Proc Natl Acad Sci U S A. 100, 342-346. Copyright © (2003) National Academy of Sciences, U. S. A.

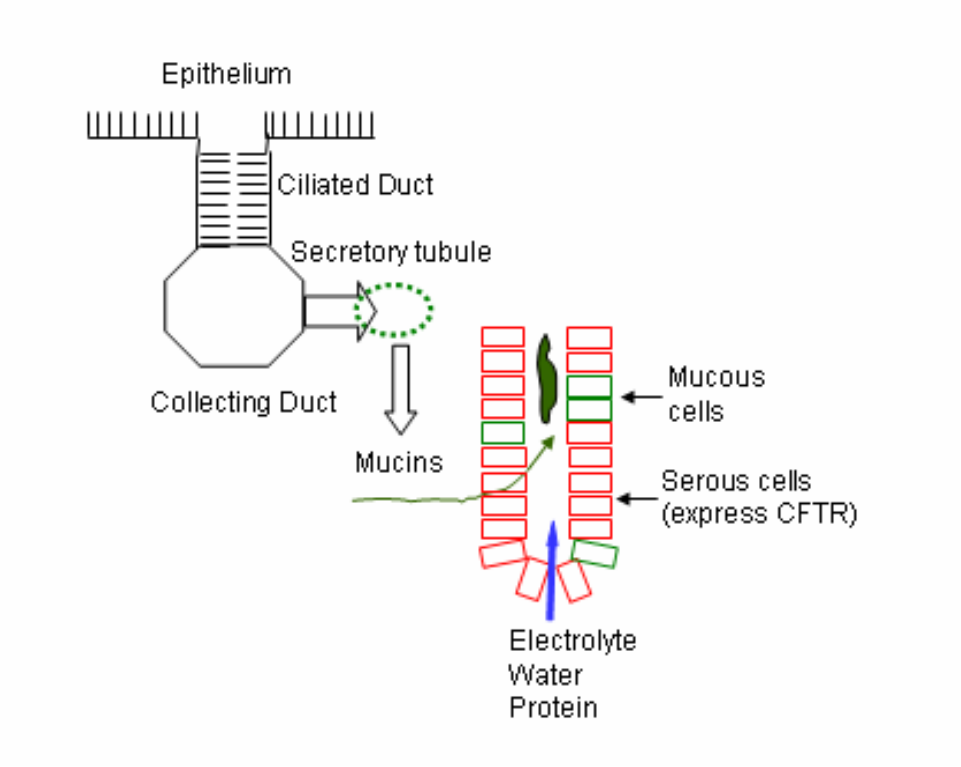

Figure 1-4. Submucosal gland structure. Modified from source: Ballard, S.T. & Spadafora, D. (2007). Fluid secretion by submucosal glands of the tracheobronchial airways. Respir Physiol Neurobiol. 159, 271-277. Copyright © (2007) Elsevier.

believed to play pivotal role in fluid secretion and transport by actively transporting chloride leading to sodium transport and thus driving osmotic water transport (Matthay et al., 2002; Matthay et al., 2005). The early evidence for defect in chloride transport in cystic fibrosis came from studies done in sweat ducts of CF patients (Quinton, 1983). Several studies later confirmed that chloride, bicarbonate and liquid transport by submucosal glands were important for lung function and the dysfunction of this transport causes CF lung pathophysiology (Inglis et al., 1998; Trout et al., 1998). Submucosal gland secretion in pig has been reported to be at least in part CFTR-dependent and this dependence has also been reported in human and mouse tracheal submucosal gland secretion (Choi et al., 2007; Ianowski et al., 2008). CF submucosal glands showed no response to VIP and forskolin when compared to healthy non-CF submucosal glands implicating an important role of CFTR in tracheal submucosal gland secretion (Wine & Joo, 2004). Also, early studies suggested that CF submucosal glands secrete thick and viscous mucus which obstruct the glands and impair mucociliary clearance thereby promoting bacterial infections (Ballard & Spadafora, 2007; Zuelzer & Newton, 1949). More recent studies using fluorescence recovery after photobleaching (FRAP) showed that the CF gland secretion was more viscous and abnormal (Salinas et al., 2005).

Airway gland secretion in disease

Diseases like chronic obstructive pulmonary disease (COPD), asthma and cystic fibrosis involve mucus hypersecretion, enlargement of submucosal glands, mucus plugs leading to obstruction, and tracheobronchial submucosal gland hypertrophy (Barnes, 1996; Fahy et al., 1992; Finkbeiner, 1999; Samet & Cheng, 1994). Although the characteristics of mucus plugs differ in asthma and COPD, they are inherent features of both these diseases (Dunnill et al., 1969; Rogers, 2003). Obstruction of airway with thick mucus and impaired mucus clearance is a major problem in airway diseases like asthma (Rogers, 2004). Owing to the central role of CFTR in serosal fluid secretion and overall fluid transport in healthy lung phenotype, it becomes mandatory to restore CFTR function in disease phenotype. Methods or substances that increase CFTR function may substantially help in restoring at least part of lung function by correcting fluid secretion and transport.

Hypothesis and Specific Aims

The unifying hypotheses of my study is that phosphodiesterase 3A (PDE3A) exists as a higher order complex, its interaction with cystic fibrosis transmembrane conductance regulator (CFTR; a PKA activated chloride channel) is regulated by cAMP, and that inhibition of PDE3A augments CFTR function.

The three specific aims of my study were to answer the questions:

- Does PDE3A inhibition increase CFTR function, can PDE3A and CFTR interact, and does PKA regulate the interaction at the plasma membrane?

- Can cAMP dynamics be monitored at the plasma membrane, and does PDE3A inhibition increase cAMP at the plasma membrane?
- Can we disrupt PDE3A-CFTR interaction, and does this alter CFTR function?

CHAPTER 2: CLONING AND PURIFICATION OF PDE3A

Materials and Methods

Cloning of PDE3A into pcDNA3.1(-)-CFP and pcDNA3.1(-)-YFP vectors

A human full length PDE3A cDNA clone was obtained from Open Biosystems (Huntsville, AL) in pCR4-TOPO vector. PDE3A was PCR amplified using Xho I and KpnI forward and reverse primers. The primers used are:

PDE3A-XhoI-Forward:
AGTCCTCGAGATGGCAGTGCCCGGCGACGCTGCACGA
PDE3A-KpnI-Reverse:
ATGCGGTACCTCACTGGTCTGGCTTTTGGGTTGGTAT

The amplified PCR product was cleaned using the Qiagen kit and eluted in 20 µL DNA grade water. The PCR cleaned sample was run on a 1% agarose gel. The product was gene cleaned using Qiagen's (Valencia, CA) QIAEX II kit. The cleaned product was ligated into pcDNA3.1 (-)-CFP and pcDNA3.1 (-)-YFP which had been restriction digested with XhoI and KpnI using Takara (Madison, WI) DNA ligation kit ver. 1, and the ligated product was transformed into DH5α cells. Six clones were picked for culture overnight; minipreps were done using Qiagen miniprep kit and the DNA was sent for sequencing to Molecular Resource Center (MRC, UTHSC). The sequence was confirmed to be pcDNA3.1 (-)-CFP-PDE3A and pcDNA3.1 (-)-YFP-PDE3A.

Ligation-independent cloning (LIC) of PDE3A into pTriEx-4 and pET-41 vectors

Human full length PDE3A and regulatory (R), catalytic, N-terminal and C-terminal domains were PCR-amplified. The PCR products were cleaned using Qiagen PCR purification kit and eluted in 20 µL DNA grade water. The PCR-cleaned DNA was further used for ligation independent cloning (LIC) using Ek/LIC cloning kit from Novagen (EMD, Gibbstown, NJ). Primers used for LIC cloning were:

PDE3A-full-length-LIC Forward:
GACGACGACAAGATGGCAGTGCCCGGCGACGCTGCACGA
PDE3A-full-length-LIC Reverse:
GAGGAGAAGCCCGGTTCACTGGTCTGGCTTTTGGGTTGGTAT
PDE3A (N-tail) 1-61 amino acid
Forward: PDE3A-full-length-LIC Forward
Reverse: GAGGAGAAGCCCGGTCTAAAGTTTCCGAGAGCTCCGGAGCGGCTG
PDE3A (R-domain) 255-750 amino acid
Forward: GACGACGACAAGATGGTGGAACAAATCTTGCCGCAGTCCGCG
Reverse: GAGGAGAAGCCCGGTCTAAGGAATATCCCTATATCCAATCTCCAA

PDE3A (Catalytic domain) 751-1035 amino acid
Forward: GACGACGACAAGATGTATCATAACAGAATCCATGCCACTGAT
Reverse: GAGGAGAAGCCCGGTCTAATCTCCTGACTCATCGCTGTCTTCCAC
PDE3A (C-tail) 1036-1141 amino acid
Forward: GACGACGACAAGATGACTGATGACCCAGAAGAAGAGGAGGAA
Reverse: PDE3A-full-length-LIC Reverse

14.6 µL of PCR-purified DNA was taken into a clean centrifuge tube and 2 µL each of 10X T4 DNA polymerase buffer and 25 mM deoxy-adenosine triphosphate (dATP) were added. 1 µL of 100 mM dithiothreitol (DTT) and 0.4 µL of T4 DNA polymerase were added to make a 20 µL total volume reaction mix. The reaction was started by adding the enzyme and stirring gently and incubated at 22°C for 30 min. The reaction was then stopped by inactivating the enzyme with 75°C incubation for 20 min. This T4 DNA polymerase-treated insert can be annealed into any Ek/LIC vectors. pTriEx-4 and pET-41 vectors were used to ligate this insert. For the ligation reaction, 1 µL Ek/LIC vector pTriEx-4 or pET-41 and 2 µL of T4 DNA polymerase-treated insert were used and incubated at 22°C for 5 min. Then, 1 µL of 25 mM EDTA was added for 5 min at 22°C. The ligated product was transformed into Novablue cells. Three clones were picked for each vector, plasmid DNA was isolated and sent for sequencing. The sequences were confirmed to be PDE3A. pTriEx-4 has a HIS-S tag whereas pET41 has a GST-HIS-S tag, and thus pTriEx-4-PDE3A with HIS-S tag and pET41-PDE3A with GST-HIS-S tags were generated. pTriEx-4 was chosen for eukaryotic expression and pET-41 for bacterial protein purification.

Generation of Flag and HA tagged PDE3A

To generate full length PDE3A with Flag or HA tag on the putative first outer loop, PDE3A was sub-cloned into pcDNA3 using XhoI and KpnI restriction enzymes. After generating pcDNA3-PDE3A construct, site-directed mutagenesis was used to insert a Flag or HA tag between amino acid position 104 and 105. Quickchange site-directed mutagenesis kit (Stratagene, La Jolla, CA) was used and mutagenic primers were designed based on the kit guidelines. The primers (forward and reverse for Flag or HA insertion) were as follows:

PDE3A-104-Flag-Forward
GAGGAGGAAGCAGCCGACTATAAAGACGACGACGACAAACCGGGAGCAGA
AGGG
PDE3A-104-Flag-Reverse
CCCTTCTGCTCCCGGTTTGTCGTCGTCGTCTTTATAGTCGGCTGCTTCCTCCTC
PDE3A-104-HA-Forward
GAGGAGGAAGCAGCCTATCCATATGACGTCCCAGACTATGCCCCGGGAGCAG
AAGGG
PDE3A-104-HA-Reverse
CCCTTCTGCTCCCGGGGCATAGTCTGGGACGTCATATGGATAGGCTGCTTCCT
CCTC

For the mutant strand synthesis reaction, 30 ng of template DNA and 125 ng each of forward and reverse primers were used in a 50 µL reaction for PCR. The amplified PCR product was treated with DpnI and transformed into XL-gold ultracompetent cells. Six clones were cultured, plasmid DNA isolated, and sent for sequencing. The sequences confirmed the presence of a Flag or HA tag at amino acid position 104 in full length PDE3A. A schematic for generation of PDE3A constructs is shown in Fig. 2-1.

Generation of HEK-293 and Calu-3 stable cell lines expressing Flag- or HA-tagged PDE3A

HEK-293 or Calu-3 cells were transfected with pcDNA3-Flag-PDE3A or pcDNA3-HA-PDE3A and selected with G418 (0.4 mg/ml) to generate stable cell lines expressing Flag or HA tagged PDE3A. HEK-293 or Calu-3 cells were plated on 60 mm dishes at a density of approximately 10^6 cells per dish. The next day, cells at about 80% confluence were transfected with pcDNA3-Flag-PDE3A or pcDNA3-HA-PDE3A or control using Lipofectamine 2000 (Invitrogen, Carlsbad, CA). About 5 µl of Lipofectamine was used for 2 µg of DNA. After 48 h, selection was started by replacing the media with media containing 0.4 mg/ml G418. Media was replaced everyday with G418 media for 2-3 weeks till colonies of stable cells survived and all other cells died. These colonies were picked by trypsinization and maintained in G418 media.

Purification of Flag-, HA-, or HIS-S-tagged PDE3A

HEK-293 cells were plated on 10 cm dishes, transfected with pcDNA3-Flag-PDE3A, pcDNA3-HA-PDE3A or pTriEx-4-PDE3A (full length or domain specific constructs) and grown for 48 h. The cells were then washed with PBS twice and lysed with PBS containing 0.2% Triton-X-100 and protease inhibitor cocktail (aprotinin, leupeptin, pepstatin and phenylmethylsulphonyl fluoride (PMSF)). The cell lysate was mixed on a shaker for 10 min at 4°C and centrifuged for 10 min at 13,000 rpm. The supernatant containing total protein was immunoprecipitated using α-Flag, α-HA beads or S-protein agarose beads overnight. The beads with bound protein were washed and the protein was eluted with 100 mM glycine (pH 2.2) and quickly neutralized with 150 mM tris (pH 8.8). The eluted protein was subjected to SDS-PAGE on 4-15% gel (Bio-Rad, Hercules, CA) and transferred to PVDF membrane and either visualized with Gel Code Blue or immunoblotted with α-Flag-HRP, α-HA-HRP or α-S-HRP antibody. A coomassie gel with purified PDE3A is shown in Fig. 2-2.

To test if we could purify large amount of fusion protein, recombinant GST-His-S-PDE3A-N-terminal protein was induced in E.coli using IPTG (0.2 mM). The fusion protein was purified using affinity chromatography (glutathione beads). The GST-fusion protein was eluted using 10 mM glutathione in TBS (pH 7.4) and was further purified using size exclusion chromatography. A chromatogram and coomassie gel for PDE3A-N-terminus is shown in Fig. 2-3.

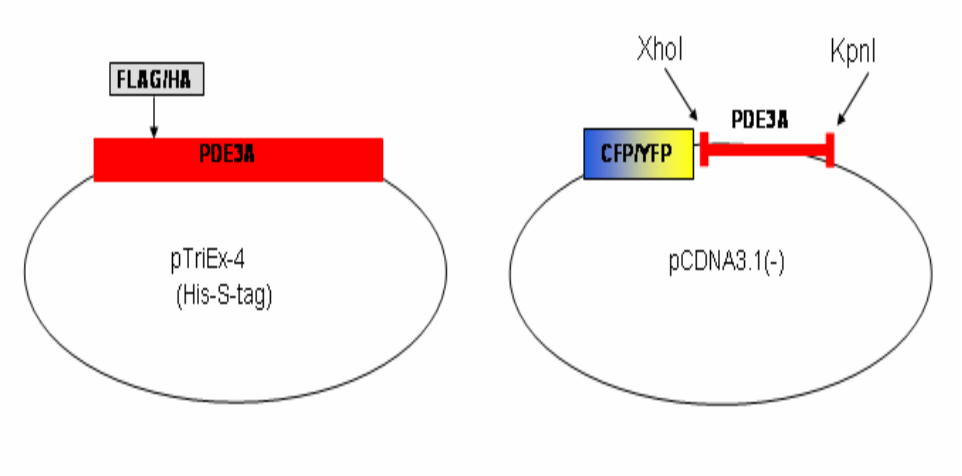

Figure 2-1. Generation of PDE3A constructs with tags

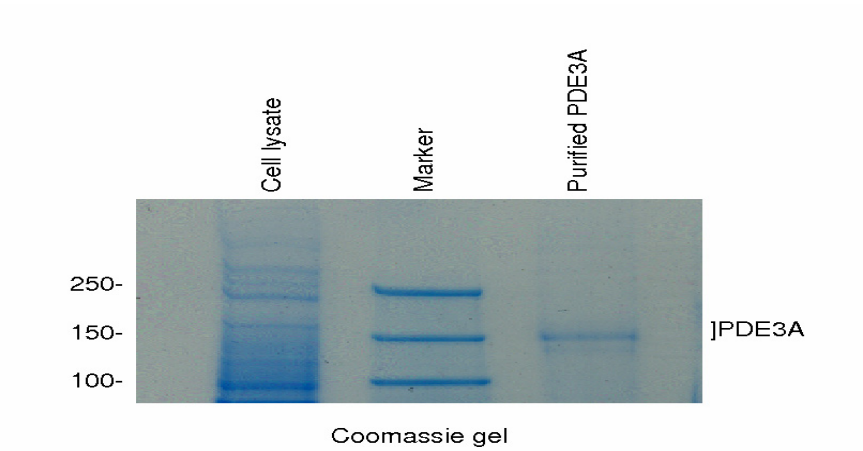

Figure 2-2. Purification of full-length PDE3A

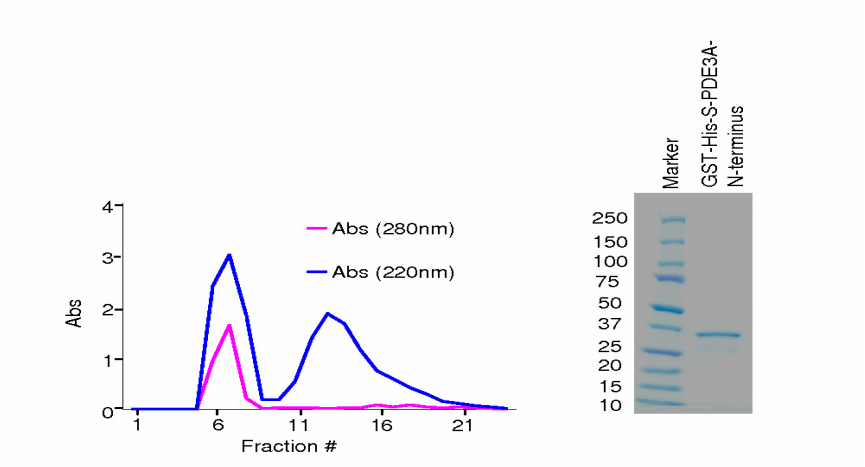

Figure 2-3. Purification of PDE3A-N-terminus

Assay for enzymatic activity of purified full length PDE3A

We used a radioactive ^{3}H-cAMP phosphodiesterase assay for measuring PDE3A enzymatic activity (Thompson et al., 1979). In the first step, PDE converts the radioactive cAMP into AMP. In the second step, nucleosidase from snake venom further converts AMP to adenosine. Ion exchange chromatography (AG® 1-X 8 resin; Bio-Rad, Hercules, CA) was used to separate cAMP and AMP from adenosine. Radioactive adenosine was measured in a scintillation counter.

Results

In this part of the study, we demonstrated the cloning and purification of PDE3A with various tags. The fluorescent CFP and YFP tags are critical to study protein-protein interactions in live cells using imaging techniques like FRET. Flag, HA, GST, HIS and S tags are crucial for biochemical studies like co-immunoprecipitation and protein purification. Generation of pcDNA3-PDE3A with various epitope tags was important for making stable cell lines. Stable cell lines expressing significant amount of PDE3A is the first and most essential requirement to carry out any biochemical studies. This is mandatory not only to purify significant amounts of protein but also to identify interacting partners. HEK-293 cells were chosen due to the ease of transfection, their human origin and response to various agonists. Also, we have HEK-293 cells stably expressing CFTR, which are known to respond to adenosine and β-adrenergic receptor agonists. We also found endogenous expression of PDE3A in HEK-293 cells by immunoblotting. This made the cell line more appealing and useful for our studies on PDE3A-CFTR interaction. Calu-3 (lung serosal epithelial cell line) on the other hand endogenously expresses both CFTR and PDE3A and also forms transepithelial membrane resistant monolayers when grown on transwell supports and thus is an ideal choice for our CFTR functional studies. Thus, we made stables of Flag-PDE3A and HA-PDE3A in both HEK-293 and Calu-3 cell lines. We purified full length PDE3A (~ 130 kDa band) from both the cell lines. To verify that the full-length protein was indeed PDE3A, we sent the purified protein out for mass spectrometry and the results identified the protein as PDE3A. Further, we purified recombinant GST-HIS-S-PDE3A domains (N-terminal, C-terminal, regulatory and catalytic) from E.coli. To confirm that the purified full-length PDE3A was functional, we used radioactive cAMP phosphodiesterase assay and found the protein had enzymatic activity when present on beads but loses activity soon after elution. We also confirmed that the insertion of Flag or HA tag on the first outer loop of PDE3A does not effect the activity of the protein.

CHAPTER 3: PDE3A AND CFTR; PHYSICAL AND FUNCTIONAL COUPLING VIA COMPARTMENTALIZED cAMP GENERATION

Materials and Methods

Reagents

Trequinsin, cilostazol and rolipram were purchased from Biomol (Plymouth Meeting, PA). Forskolin was obtained from Tocris (Ellisville, MO). Isoproterenol was purchased from Calbiochem (EMD, Gibbstown, NJ). DSP was obtained from Pierce (Thermo Fisher, Rockford, IL). Adenosine, IBMX, cpt-cAMP, latrunculin B, carbachol, and indomethacin were purchased from Sigma-Aldrich (St. Louis, MO).

Cell culture and transfections

HEK293 cells were cultured in DMEM-F12 media containing 10% serum and 1% penicillin/streptomycin and maintained in a 5% CO_2 incubator at 37^{o}C. Calu-3 cell line was purchased from ATCC (Manassas, VA) and cultured in MEM media containing 15% serum, 1% penicillin/streptomycin, 1 mM sodium pyruvate and 1X non-essential amino acids. Lipofectamine 2000 was used to express plasmids containing CFTR or PDE3A in both HEK293 and Calu-3 cell lines according to the manufacturer's instructions. Stable cell lines were generated by selection using 0.4 mg/ml G418 (geneticin).

Short circuit current (I_{SC}) measurements

Polarized lung serosal cells (Calu-3) monolayers were grown on Costar Transwell permeable supports (filter area 0.33cm^2) until the monolayer reached a resistance of ~1500 ohms and the transwell was mounted in an Ussing chamber. Short circuit currents were measured as described previously (Li et al., 2005). Epithelia were bathed in Ringer's solution (mM) (Basolateral: 140 NaCl, 5 KCl, 0.36 K_2HPO_4, 0.44 KH_2PO_4, 1.3 $CaCl_2$, 0.5 $MgCl_2$, 4.2 $NaHCO_3$, 10 HEPES, 10 glucose, pH 7.2, [Cl^-] = 149), and low Cl^- Ringer's solution (mM) (Apical: 133.3 Na-gluconate, 5 K-gluconate, 2.5 NaCl, 0.36 K_2HPO_4, 0.44 KH_2PO_4, 5.7 $CaCl_2$, 0.5 $MgCl_2$, 4.2 $NaHCO_3$, 10 HEPES, 10 mannitol, pH 7.2, [Cl-] = 14.8) at 37°C, and saturated with 95% O_2 and 5% CO_2. The monolayers were bathed in a low chloride Ringer's solution on the apical side and normal Ringer's solution on the basolateral side. A 2 mV pulse was applied every 1 min throughout the experiment to check for the integrity of the epithelia. PDE3-specific inhibitor cilostazol (10-100 μM) was added to apical and basolateral sides. Forskolin (20 μM) was added to both sides for maximal response. CFTRinh-172 (20 μM) was added to the apical side. For I_{SC} measurements with actin cytoskeleton disruption of the cells, latrunculin B (1 μM) was added to both apical and basolateral sides after pre-treating the cells with latrunculin B (1 μM) for 30 min.

Membrane preparation and immunoblotting

For detecting PDE3A expression and localization in cells using Western blotting, crude membrane and cytosolic fractions were isolated. In order to prepare crude membrane and cytosol, HEK-293 parental cells, Calu-3 cells or Calu-3 cells transfected with HA-PDE3A were grown on 10 cm dishes. The dishes were washed with PBS and scraped in PBS and the cells pelleted at 600 g for 5 min at 4°C. The pellet was then resuspended by incubation with hypotonic lysis buffer (10 mM HEPES, 1 mM EDTA, protease inhibitor cocktail, pH 7.2) for 10 min before lysis by 10 strokes in Dounce homogenizer, followed by 15 strokes in the presence of equal volume of sucrose buffer (500 mM sucrose, 1 mM EDTA, 10 mM HEPES, pH 7.2). The lysate was spun at 6000 g for 20 min at 4°C to obtain post-mitochondrial supernatant. Crude membrane was collected by centrifuging the supernatant at 100,000 g for 45 min at 4°C. The pellet was resuspended in isotonic buffer (250 mM sucrose, 1 mM EDTA, 10 mM HEPES, pH 7.2) to collect crude membrane and supernatant was used for cytosolic fraction. The protein was mixed with Laemmli sample buffer (5x; containing 2.5% β-mercaptoethanol), denatured, subjected to SDS-PAGE on 4-15% gel and transferred to PVDF membrane. PDE3A mAb from Novus Biologicals (Littleton, CO) was used for immunoblotting.

Coimmunoprecipitation and immunoblotting

Cells transfected with Flag-CFTR and HA-PDE3A or only HA-PDE3A were lysed using lysis buffer (1x PBS, containing 0.2% Triton-X-100 and protease inhibitors phenylmethylsulfonyl fluoride 1 mM, pepstatin-A 1 µg/ml, leupeptin 1 µg/ml, aprotinin 1 µg/ml). The lysate was centrifuged at 16,000 g for 10 min at 4 ºC and the clear supernatant was subjected to immunoprecipitation using α-Flag beads (Sigma-Aldrich, St.Louis, MO). The immunoprecipitated beads were washed three times with lysis buffer and the protein was eluted from the beads using Laemmli sample buffer (5x; containing 2.5% β-mercaptoethanol). The eluates were denatured and subjected to SDS-PAGE on 4-15% gel. The protein was transferred to PVDF membrane. PDE3A mAb from Novus Biologicals (Littleton, CO) was used for immunoblotting.

Cross-linking the complex and immunoblotting

Thiol-cleavable, amine-reactive, homobifunctional cross-linker dithiobis succinimidyl propionate (DSP, 1 mM) was used to cross-link protein complex in HEK-293 cells grown on 10 cm dishes expressing both Flag-CFTR and HA-PDE3A. HEK-293 cells expressing only Flag-CFTR were used as control. The cells were pre-treated with 1 µM latrunculin B for 30 min at 37°C and then cross-linked with 1 mM DSP for 5 min at 37°C. The reaction was quenched by lysing the cells with ice-cold RIPA buffer (140 mM NaCl, 1% Nonidet P40, 0.5% Na-deoxycholate, 0.1% Na-dodecyl sulphate and 50 mM Tris-HCl, pH 8.0) containing protease inhibitor cocktail. The supernatant was spun at 20,000 rpm for 10 min. After taking 100 µL of total protein for input, the rest of the protein was immunoprecipitated by adding α-HA beads overnight. The beads were

washed twice with RIPA buffer and the cross-linked complex was eluted with 100 mM glycine (pH 2.2) and quickly neutralized with 150 mM Tris (pH 8.8). For cleaving the disulphide bond of DSP and separating the proteins, 2.5% β-mercaptoethanol was added to the sample Laemmli buffer. The eluted proteins were mixed with Laemmli sample buffer (5x; containing 2.5% β-mercaptoethanol), denatured, subjected to SDS-PAGE, transferred to PVDF membrane and immunoblotted using α-M3A7-CFTR antibody from Millipore (Billerica, MA).

Surface biotinylation and immunoblotting

Cells expressing HA-PDE3A were surface biotinylated with EZ-Link Sulfo-NHS-LC-Biotin from Pierce (Rockford, IL) for 1 h at 4°C, lysed, and immunoprecipitated using α-HA agarose beads (Sigma-Aldrich, St.Louis, MO). The biotinylated purified HA-PDE3A was pulled down using streptavidin beads (Pierce, Rockford, IL) for 1 h at room temperature. The beads were spun down to collect unbound fraction, and the beads contained the bound fraction. The samples were mixed with Laemmli sample buffer (5x; containing 2.5% β-mercaptoethanol), denatured, subjected to SDS-PAGE on 4-15% gel, transferred to PVDF membrane and immunoblotted with α-PDE3A mAb from Novus Biologicals (Littleton, CO).

FRET microscopy and data analysis

For ratiometric FRET, HEK 293 cells expressing CFP-EPAC-YFP were grown on glass-bottom dishes (MatTek, Ashland, MA), washed twice with Hank's balanced salt solution (HBSS) and mounted on an inverted Olympus wide-field microscope (IX51, U-Plan Fluorite 60x 1.25 NA oil-immersion objective) for FRET imaging. The stage was maintained at 37°C constantly and the cells were maintained in the dark in HBSS. After establishing the baseline, PDE inhibitors were added as indicated. Ratiometric FRET imaging was performed as described previously (Li et al., 2007). Time-lapse images were obtained with 1x1 binning, 100-300 ms exposure time and 1 min intervals. Images were acquired using an EM CCD camera (Hamamatsu) mounted on an Olympus IX51. The light source used was 300W xenon lamp with a neutral density filter. A JP4 CFP/YFP filter set was used for image capture (Chroma, Brattleboro, VT) which includes a 430/25 nm excitation filter, a double dichroic beam splitter and two emission filters (470/30 nm for CFP and 535/30 nm for FRET emission) alternated by filter-change controller Lambda 10-3 (Sutter instruments, Novato, CA). Slidebook 4.2 software was used for data analysis. Following background subtraction, multiple regions of interest (10-20) were selected (3-5 cells) for data analysis using ratio module. The emission ratio (CFP/FRET) was obtained from CFP and FRET emission of background subtracted cells.

For direct sensitized emission FRET, HEK 293 cells were transiently transfected with pCDNA3-CFP-PDE3A or pCDNA3-YFP-CFTR or both using Lipofectamine 2000. Single transfected cells were used to acquire CFP or YFP only images for bleed through calculations. Double transfectants were used for data collection using CFP/YFP filter

sets. The cells were split at low density at 20-40% confluence into a cover slip bottom dish (MatTek; Ashland, MA), washed twice with warm HBSS and 2 ml of HBSS was added. Cells were imaged in a dark room at 37°C. After acquiring images without PKA agonists as 0 time point images, PKA activating cocktail (Forskolin 10 μM, IBMX 100 μM, cpt-cAMP 200 μM) was added and images were acquired at 2, 4, 6, 8 and 10 min intervals. Corrected FRET was calculated on a pixel-by-pixel basis for the entire image by using equation: FRETc = FRET - (0.5 × CFP) - (0.06 × YFP), where FRET, CFP, and YFP correspond to background-subtracted images of cells co-expressing CFP-PDE3A and YFP-CFTR acquired through the FRET, CFP, and YFP channels, respectively (Galperin & Sorkin, 2003). The factors 0.5 and 0.06 are the fractions of bleed-through of CFP and YFP fluorescence, respectively, through the FRET filter channel. The corrected FRET (FRETc) was normalized with donor CFP intensity (FRETc/CFP), yielding the normalized corrected FRET (N-FRETc), and the intensity of N-FRETc images was presented in monochrome mode, stretched between the low and high renormalization values, according to a intensity to color mapped lookup table with black indicating low values and white indicating high values. All calculations were performed using the Channel Math and FRET modules of the SlideBook 4.2 software (Intelligent Imaging Innovations; Denver, CO).

Single particle tracking

Calu-3 cells stably expressing HA-PDE3A were grown on 35 mm glass bottom dishes (MatTek, Ashland, MA). Cells were washed twice with phosphate buffered saline containing 6 mM glucose and 1 mM sodium pyruvate (PBS/Glu/NaPyr) and blocked with PBS/Glu/NaPyr containing 4% bovine serum albumin (BSA) for 10 min. Cells were then incubated with biotin α-HA antibody (1 μg/ml, Sigma-Aldrich, St. Louis, MO) for 15 min, washed five times, followed a second incubation with streptavidin-conjugated Qdot-655 (0.1 nM, Invitrogen, Carlsbad, CA) for 2 min, washed 8 times, and immediately mounted on an Olympus inverted microscope (IX51), and the images were captured with Hamamatsu EM-CCD camera at 1-3 frames per second (fps) for 1-3 min with 50 ms exposure time, 100x oil-immersion objective (NA 1.40), xenon (300W lamp) light source, and SlideBook 4.2 software. Qdot 655-A BrightLine® high brightness and contrast single band filter set (Semrock, Rochester, NY) was used for collecting data. Single particle tracking was done using particle tracking module of SlideBook 4.2 software, which generates trajectories and also calculates MSD. Diffusion coefficient (D) was calculated by linear squares fitting using points 1-5 on the MSD curve. 5-10 cells were used for plotting histograms of diffusion coefficient. To monitor changes in diffusion with cytoskeletal disruption, cells were pre-treated with latrunculin B (1 μM, 30 min) and latrunculin B was also added to the buffer during the course of the experiment.

Submucosal gland secretion

Submucosal gland secretion was monitored and analyzed as described by Wine's laboratory (Joo et al., 2001). Freshly collected pig trachea was placed in cold Krebs-Ringer bicarbonate buffer (120 mM NaCl, 25 mM $NaHCO_3$, 3.3 mM KH_2PO_4, 0.8 mM K_2HPO_4, 1.2 mM $MgCl_2$, 1.2 mM $CaCl_2$, 10 mM D-glucose and 1 μM indomethacin). The submucosal layer was carefully dissected from the cartilage and a 1 cm piece was mounted in a chamber mucosal side up. The mucosal side was wiped and quickly air-dried with 95% O_2 and 5% CO_2 gas. A thin layer of water-saturated mineral oil was applied to the mucosal side. The tissue was constantly maintained at 37°C and gassed with 95% O_2 and 5% CO_2 after mounting. To establish a baseline, Krebs-Ringer bicarbonate buffer was added to the serosal side. PDE3 inhibitor cilostazol, CFTR inhibitor 172 and latrunculin B (10 μM) were added to the serosal side after monitoring basal secretion. Carbachol was added at the end of the experiment to check for the viability of submucosal glands. Images were collected at 1 min time intervals with a digital camera (Motic Images 2.0 ML software, National Optical, San Antonio, TX) attached to a stereoscopic microscope (National Optical, San Antonio, TX) and analyzed using ImageJ software (NIH, Bethesda, MD). A 1 mm x 1 mm grid was placed on the tissue in the last image for area measurements. Volume was calculated from area using the formula $v = \Pi r^3$ and rate was calculated as slope of volume vs. time plot by fitting at least four points using linear regression.

Surface labeling assay

Cells expressing Flag or HA-PDE3A grown on 35 mm dishes were fixed with 3.7% formaldehyde for 10 min, blocked with 1% BSA for 30 min, and treated with α-Flag or HA-HRP (0.2 μg/ml) for 90 min. HRP substrate 1-step Ultra TMB (Pierce, Rockford, IL) was added to the dishes for about 10-20 min, and the reaction was stopped by adding equal amount of 2 M H_2SO_4 and the absorbance was read at 450 nm. To detect any altered surface expression with PKA phosphorylation, cells were pre-treated with forskolin (20 μM) for 10 min, fixed, surface labeled and then assayed. To detect the effects of latrunculin B on PDE3A surface expression levels, Calu-3 cells expressing HA-PDE3A were pre-treated with latrunculin B (1 μM) for 30 min and then proceeded for surface labeling as described above.

Iodide efflux assay

CFTR mediated halide efflux was measured using iodide efflux assay. HEK-293 cells expressing wild type CFTR were grown on 60 mm dishes, and iodide efflux was assayed as described. Briefly, cells were loaded for 60 min at room temperature with loading buffer (136 mM NaI, 137 mM NaCl, 4.5 mM KH_2PO_4, 1 mM $CaCl_2$, 1 mM $MgCl_2$, 10 mM glucose, 5 mM HEPES, pH 7.2). Extracellular NaI was washed away thoroughly (5 times) with efflux buffer (136 mM $NaNO_3$ replacing 136 mM NaI in the loading buffer) and cells were equilibrated for 1 min in a final 1 ml aliquot. The first four

aliquots were used to establish a stable base line in efflux buffer alone. Agonist (1 μM adenosine with or without 100 μM cilostazol or 5 μM isoproterenol with or without 20 μM trequinsin) was added to the efflux buffer and samples were collected every 1 min for 6 min in the continued presence of agonists (i.e., the efflux buffer used for subsequent replacements also contained agonists at the same concentration). The iodide concentration of each aliquot was determined using an iodide-sensitive electrode (Thermo Scientific, Waltham, MA) and converted to iodide content (nanomoles/min). HEK 293 parental cells in the presence of agonist forskolin were used as a negative control.

Immunofluorescence

Calu-3 cells on glass-bottom dishes were directly used after fixing with 3.7% formaldehyde or paraffin embedded pig trachea was processed for immunostaining. Paraffin embedded pig trachea was sectioned. The slides with sections were treated with protease to retrieve the antigen. The cells on dishes and antigen retrieved sections were blocked with PBS with 4% BSA and 0.2% Triton-X-100, inside a humidifying chamber for 2 h. The slides or dishes were treated with rabbit polyclonal α-PDE3A from Santa Cruz Biotechnology (Santa Cruz, CA) at 1:50 dilution overnight. Normal rabbit IgG was used for negative control. The slides were treated for 1 h with secondary antibody α-rabbit AlexaFluor 488 (Molecular probes, Invitrogen, Eugene, OR) at 1:500 dilution and 1:1000 dilution of propidium iodide. Images were taken on a Carl-Zeiss (Thornwood, NY) confocal microscope. For co-localization experiments, rabbit polyclonal α-PDE3A and mouse monoclonal α-CFTR primary antibodies were used and AlexaFuor 488 and 568 secondary antibodies were used. Normal rabbit and mouse IgG were used for negative control. Calu-3 cells were fixed for 30 min at -20°C using acetone-methanol and further fixed with 3.7% formaldehyde.

AlphaScreen™ for PDE3A-CFTR interaction

We used AlphaScreen™ (Amplified Luminescent Proximity Homogeneous Assay) to study CFTR-PDE3A interaction. Purified full-length Flag tagged CFTR and biotinylated HA-PDE3A were used and 2103 EnVision multilabel plate reader was used to measure the fluorescence between acceptor and donor beads. AlphaScreen™ FLAG™ (M2) detection kit was used to detect the interaction between purified full-length biotin-(HA)-PDE3A and Flag-(M2)-wt-CFTR. In brief, starting from 100 nM final concentration, biotin-(HA)-PDE3A was serially diluted (in 1/2 log dilution series) in assay buffer [1x PBS, 0.1% BSA, 0.05% Tween 20 (v/v), pH 7.2] containing Flag-wt-CFTR (100 nM final concentration). The resulting solutions were incubated at room temperature for 30 min. Each sample solution (15 μl) was transferred to a white opaque 384-well microplate (OptiPlateTM-384, PerkinElmer, MA) in triplicates and into which anti-FLAG (M2) acceptor beads (5 μl, 20 μg/ml final concentration) were added and incubated for 30 min at room temperature. Streptavidin donor beads (5 μL, 20 μg/ml final concentration) were then added and incubated for 2 h at room temperature. The plate was

read on an EnVisionTM 2103 Multilabel Reader (PerkinElmer, MA) or FLUOstar-Omega plate reader with AlphaScreen™ capability (BMG labtech, Durham, NC).

Cell-attached single-channel recording

Single-channel recordings were obtained from Calu-3 cells as described previously (Li et al., 2007). The pipette solution contained either forskolin or cilostazol (10-20 μM) to activate CFTR channels. Both bath and pipette solution contained (in mM) 140 N-methyl-D-glucamine, 140 HCl, 2 $CaCl_2$, 2 $MgCl_2$, 10 HEPES, pH 7.4. Single channel currents were recorded at a test potential of +80 mV (reference to the cell interior) delivered from the recording electrode, and were filtered at 100 Hz and sampled at 2 kHz.

Statistical analyses

Statistical analyses were done using Student's t-test (2-tailed) or ANOVA (single-factor), and $p < 0.01$ or $p < 0.05$ was considered significant. All the results are represented as mean $\pm$ SEM with n being the number of experiments.

Results

PDE3A inhibition augments CFTR function by generation of compartmentalized cAMP

Submucosal glands secretion plays important roles in maintaining airway and lung health. It is usually stimulated by agonists that elevate cAMP or Ca^{2+} level and has been reported to be at least in part CFTR-dependent (Choi et al., 2007; Ianowski et al., 2008). To explore the physiological relevance of functional coupling between CFTR and PDE3A, we used pig tracheal submucosal gland secretion model. Pig is considered a closer model to human cystic fibrosis (CF), and a CF pig model is available for studying CFTR function (Rogers et al., 2008). After established basal secretion, a specific PDE3 inhibitor, cilostazol (100 μM), was added to the serosal side to inhibit PDE3A. Cilostazol has been approved for treatment of intermittent claudication since 1999 in the USA and for treatment of peripheral artery occlusive disease (PADO) in Japan since 1988 (Thompson et al., 2007). As shown in Fig. 3-1, upon PDE3A inhibition, we observed a 3-fold increase in mean mucosal secretion rate (from 0.5 nl/min/gland basal secretion rate to 1.5 nl/min/gland). This increased secretion was inhibited by treatment of the trachea with a specific CFTR channel inhibitor, CFTRinh-172 (50 μM), suggesting that the increased secretion is CFTR-dependent. Carbachol, an agonist which stimulate the glands secretion by elevating Ca^{2+} level, was added at the end of the experiments to check for the viability of submucosal glands (Fig. 3-1).

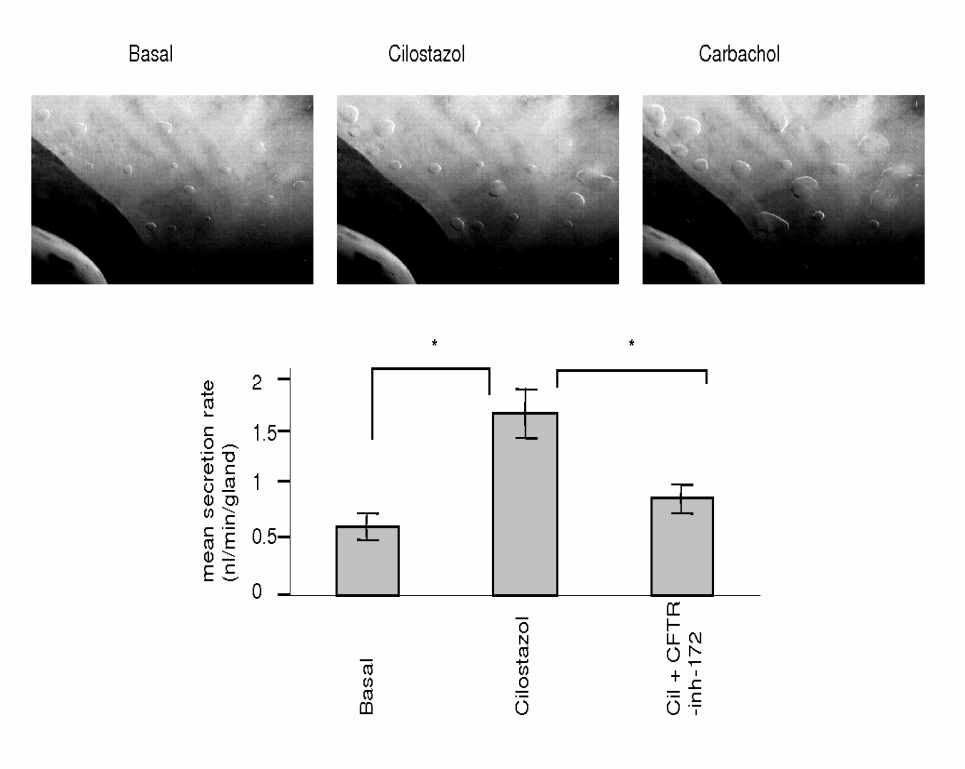

Figure 3-1. CFTR dependent submucosal gland secretion increases with PDE3A inhibition

The expression and localization of PDE3A in pig trachea was studied by immunohistochemical analysis using a PDE3A-specific antibody and α-rabbit AlexaFluor 488 as the secondary antibody. We also investigated the localization of PDE3A in Calu-3 cells, a widely used model for submucosal gland serous cells (Ianowski et al., 2008). Non-immune rabbit IgG was used as a negative control in these studies. As can be seen in Fig. 3-2, PDE3A is primarily localized at the plasma membrane of epithelial cells of pig trachea and at the plasma membrane of Calu-3 cells. It is to be noted that CFTR is also expressed at the plasma membrane of Calu-3 cells (Li et al., 2004; Li et al., 2005; Naren et al., 2003). We also used immunofluorescence to detect co-localization between PDE3A and CFTR endogenously. Calu-3 cells showed co-localization of PDE3A and CFTR (Fig. 3-2).

To investigate if the functional coupling of PDE3A and CFTR can be observed in live cells, we used two CFTR Cl^- channel function assays. The first one was to measure CFTR-dependent short circuit current (I_{SC}) in polarized Calu-3 cells mounted in an Ussing chamber (Li et al., 2007). Consistent with the observation of Drumm's group (Kelley et al., 1995), PDE3A inhibition increased CFTR Cl^- channel function. In the presence of PDE3 inhibitors trequinsin (1-20 μM) or cilostazol (10-100 μM), we observed a dose-dependent increase in CFTR-mediated currents which was inhibited by CFTRinh-172 (20 μM) (Fig. 3-3). Forskolin (20 μM), a adenylyl cyclase stimulator which elicits a global increase of cAMP and maximally stimulates CFTR function (Li et al., 2005; Li et al., 2007), was used as positive control for these studies. It is to be noted that inhibition of PDE3A induced smaller magnitude of I_{SC} response compared to that stimulated by forskolin (20 μM). In the case of using cilostazol, the I_{SC} could be further increased to a maximal level by using forskolin (20 μM) suggesting that inhibition of PDE3A generates localized cAMP rather than global cAMP.

The second CFTR functional assay we used was to measure the iodide efflux from HEK293 cells overexpressing Flag-wt-CFTR. Adenosine or isoproterenol were used to activate CFTR channel function in these studies and HEK293 parental cells stimulated by forskolin were used as negative control. As can be seen in Fig. 3-4, inhibition of PDE3A increased CFTR-mediated iodide efflux. In the presence of cilostazol (100 μM), the iodide efflux increased > 50% when a low dose of adenosine (1 μM) was used. Similarly, by using trequinsin (20 μM), the iodide efflux increased > 50% when a low dose of isoproterenol (5 μM) was used. Adenosine is a cAMP-elevating ligand which has been reported to stimulate CFTR channel function in a compartmentalized manner at the apical cell membranes when being used at low (< 20 μM) concentrations (Huang et al., 2001; Li et al., 2007). Isoproterenol is a β adrenergic receptor (β-AR) agonist which acts via activation of β-AR and AC to induce cAMP.

The expression and localization of PDE3A in HEK293 cells and Calu-3 cells was studied by Western blotting. Calu-3 cells transfected with HA-PDE3A were used as positive control (Fig. 3-5). The results show that PDE3A is expressed in the membrane of these cells.

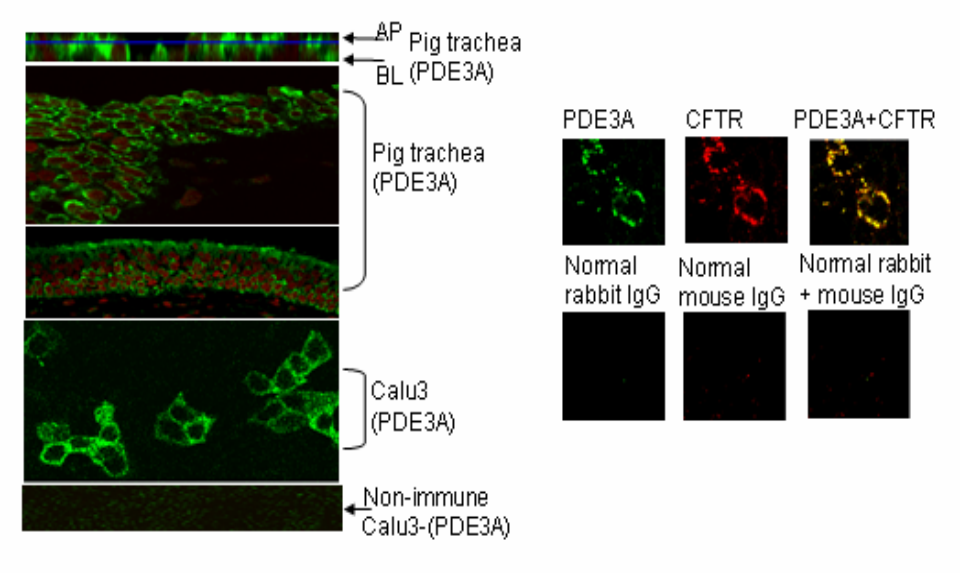

Figure 3-2. Immunofluorescence and co-localization of PDE3A

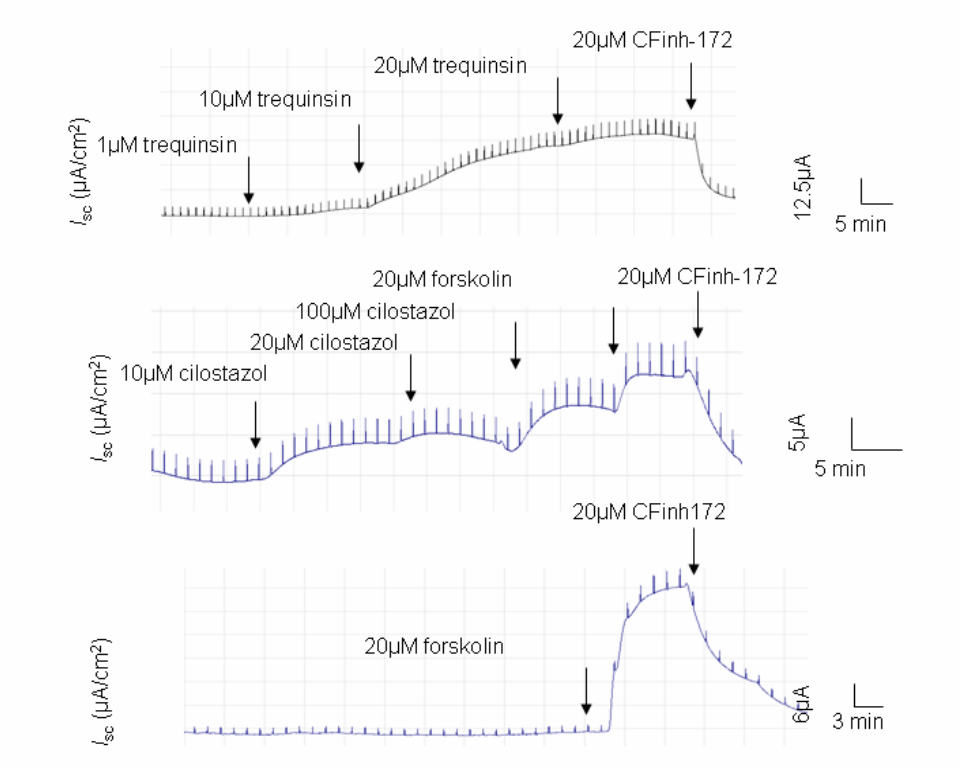

Figure 3-3. Ussing chamber data shows PDE3 inhibition augments CFTR function

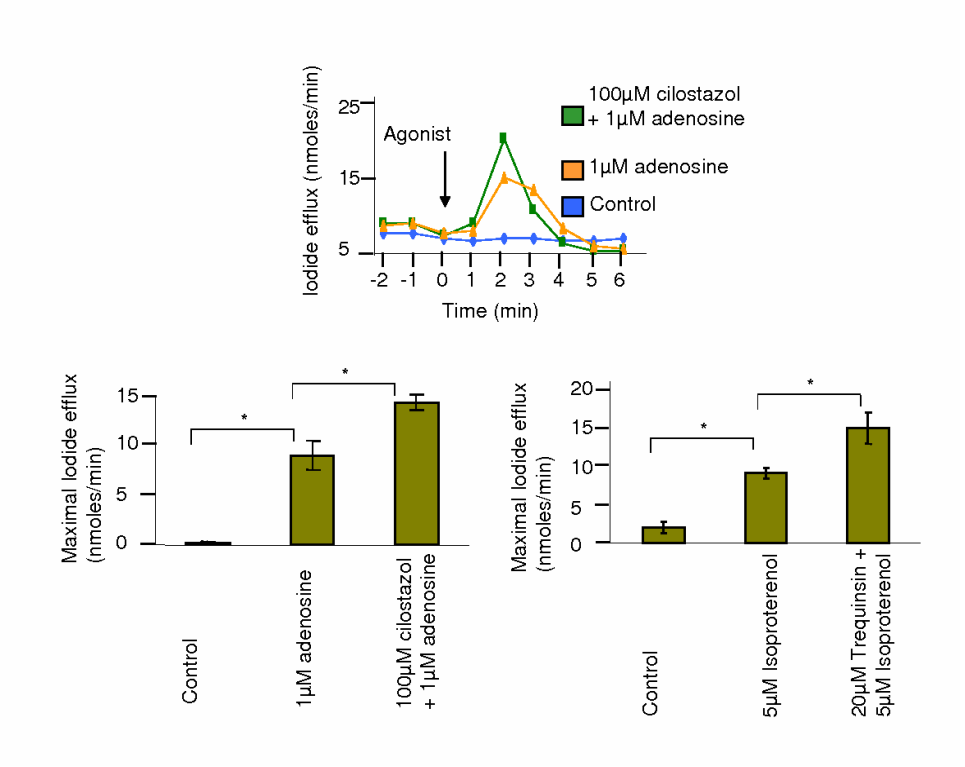

Figure 3-4. Iodide efflux assay shows HEK-293-Flag-CFTR cells show increased CFTR function with PDE3 inhibition

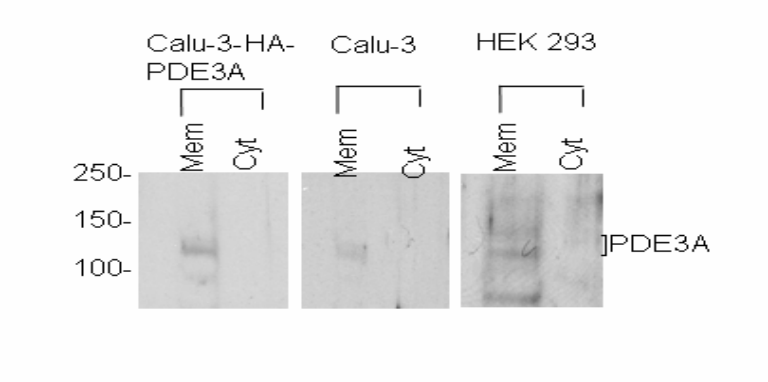

Figure 3-5. PDE3A is expressed in the membrane of HEK-293 and Calu-3 cells

To further characterize the localization of cAMP upon PDE3A inhibition and to investigate the possible mechanism through which CFTR functionally couples to PDE3A, a FRET-based cAMP sensor, CFP-EPAC-YFP, was transfected into HEK293 cells and then subjected to ratiometric fluorescence resonance energy transfer (FRET) measurements. This highly sensitive, unimolecular fluorescent cAMP indicator allows to monitor cAMP dynamics in intact cells with very high temporal and spatial resolution (Li et al., 2007; Ponsioen et al., 2004). As can be seen from Fig. 3-6, upon PDE3A inhibition by using cilostazol, cAMP levels (represented by CFP/FRET emission ratio) increased in a dose-dependent manner. More importantly, the increase of cAMP levels occurs mainly at the edge area of the cells, suggesting a highly compartmentalized cAMP accumulation at the plasma membrane. Interestingly, addition of a PDE4 inhibitor, rolipram (10μM), induced a global increase in cAMP levels (indicated by the uniform increase of the emission ratio in the entire cytoplasm) which is similar to the effect seen with forskolin stimulation (20μM; Fig. 3-7). It seems reasonable to propose that in these cells PDE3A is probably involved in compartmentalized cAMP signaling whereas PDE4 regulates global cAMP levels. Taken together, our data showed that PDE3A is functionally coupled to CFTR. Inhibition of PDE3A augments CFTR function by generation of highly compartmentalized cAMP.

PDE3A interacts with CFTR in a PKA-dependent manner

Given the evidence of functional coupling, we continued to investigate whether a physical coupling between PDE3A and CFTR existed. Towards this, we co-transfected HEK293 cells with CFP-PDE3A and YFP-CFTR and measured the direct sensitized emission FRET in live cells. A schematic diagram of FRET assay is shown in Fig. 3-8. As shown in Fig. 3-9, the two proteins interacted at the plasma membrane as indicated by the FRET signals. More importantly, this interaction increased by almost 70% (normalized FRET) upon treatment with a PKA-activating cocktail (forskolin 10 μM, IBMX 100 μM, and cpt-cAMP 200 μM), suggesting that the interaction between CFTR and PDE3A is PKA-dependent. Phosphorylation increases the binding between PDE3A and CFTR. To confirm that CFP and YFP do not show FRET by themselves, we transfected cells with CFP and YFP only and observed that there was no significant FRET between the fluorophores (Fig. 3-10).

Coimmunoprecipitation and immunoblotting were also used to detect the interaction between PDE3A and CFTR. HEK293 cells were co-transfected with HA-PDE3A and Flag-CFTR, immunoprecipitated using α-Flag beads and immunoblotted for PDE3A. Cells transfected with HA-PDE3A were used as negative control. For all the protein interaction studies, we generated PDE3A constructs with either Flag or HA tag on the first outer loop at position 104 and CFTR with Flag tag at position 901 on the fourth outer loop (Fig. 3-11). As shown in Fig. 3-12, HA-PDE3A can be coimmunoprecipited with Flag-CFTR, suggesting interaction exists between these two proteins which corroborate the FRET data.

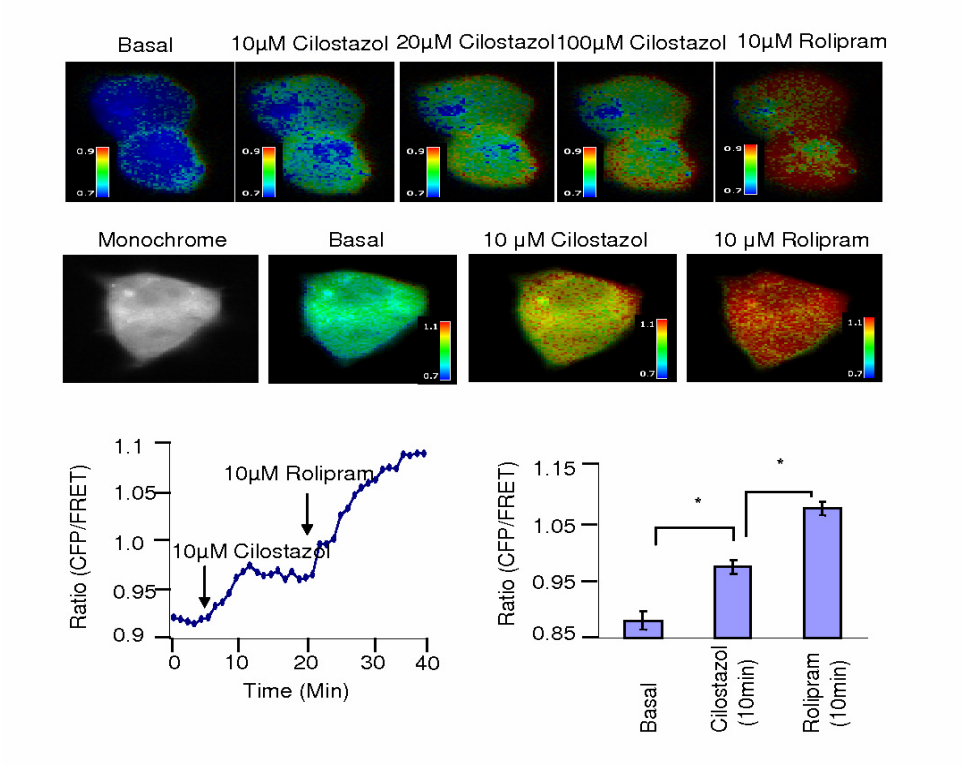

Figure 3-6. Compartmentalized cAMP is generated with PDE3 inhibition

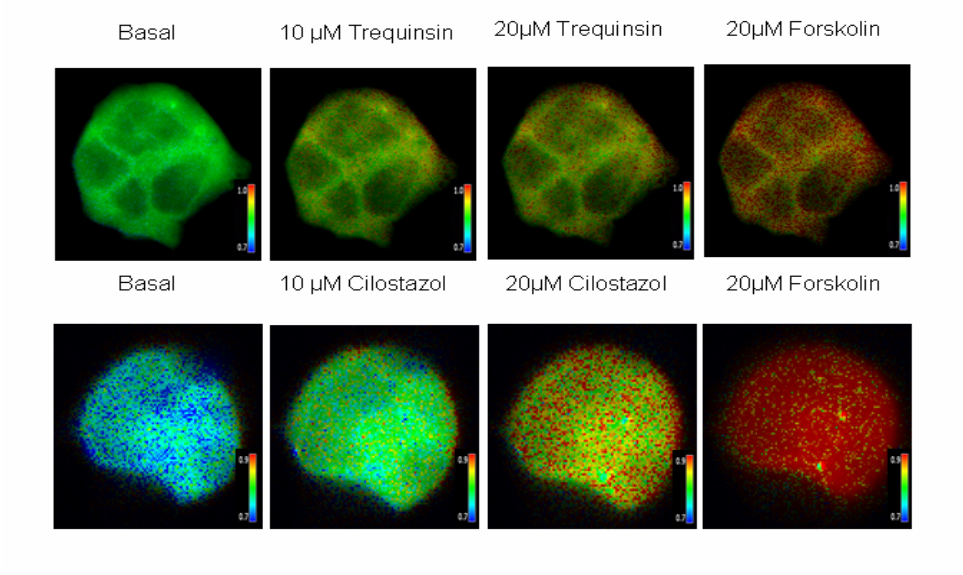

Figure 3-7. PDE3 inhibition generates local cAMP whereas forskolin generates global cAMP

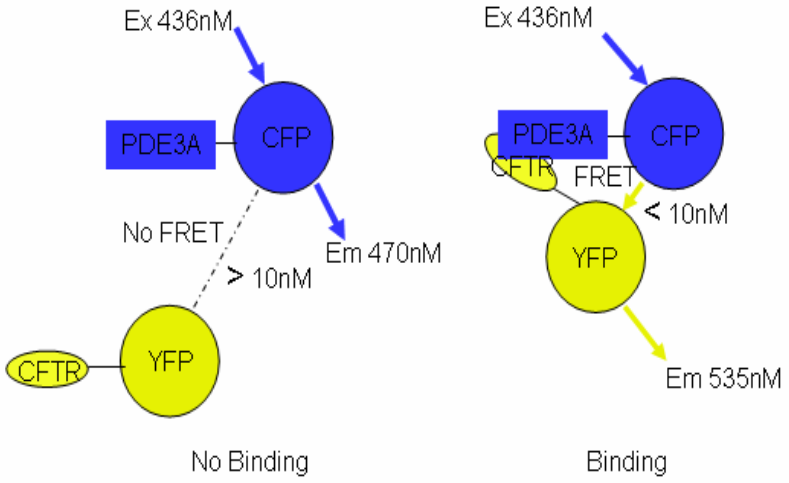

Figure 3-8. Schematic diagram for FRET

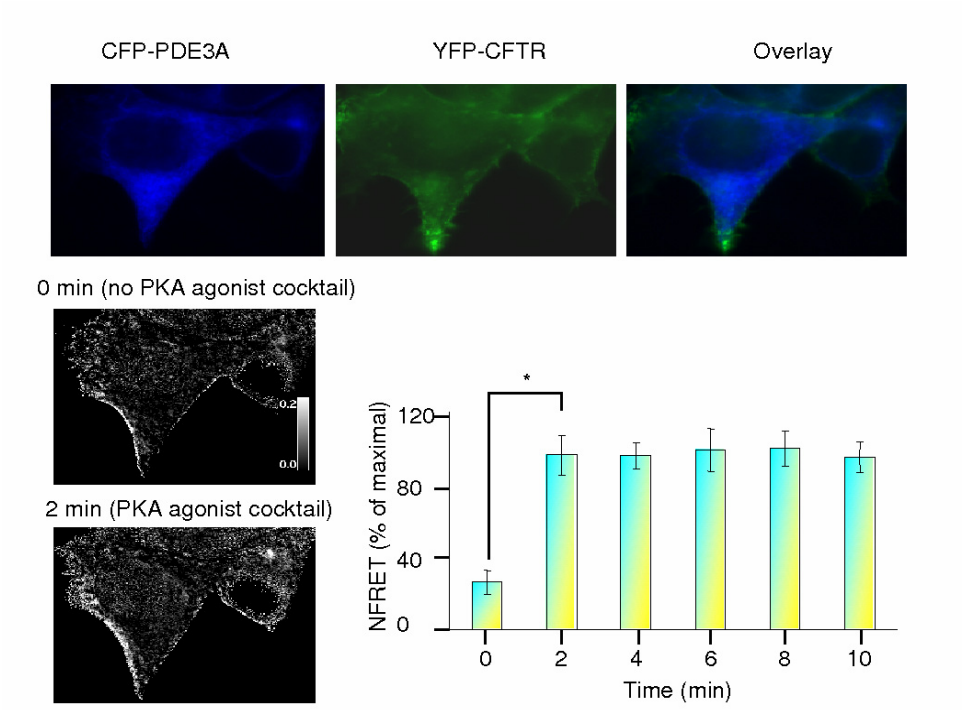

Figure 3-9. FRET reveals interaction between CFTR and PDE3A in live cells

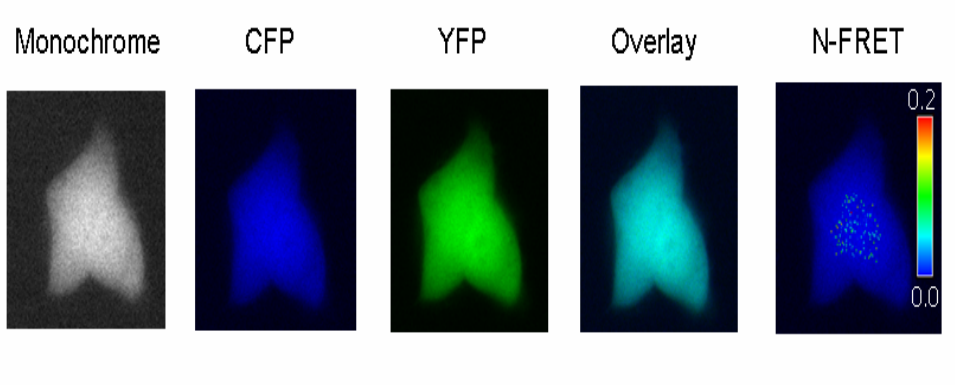

Figure 3-10. CFP and YFP by themselves do not show FRET

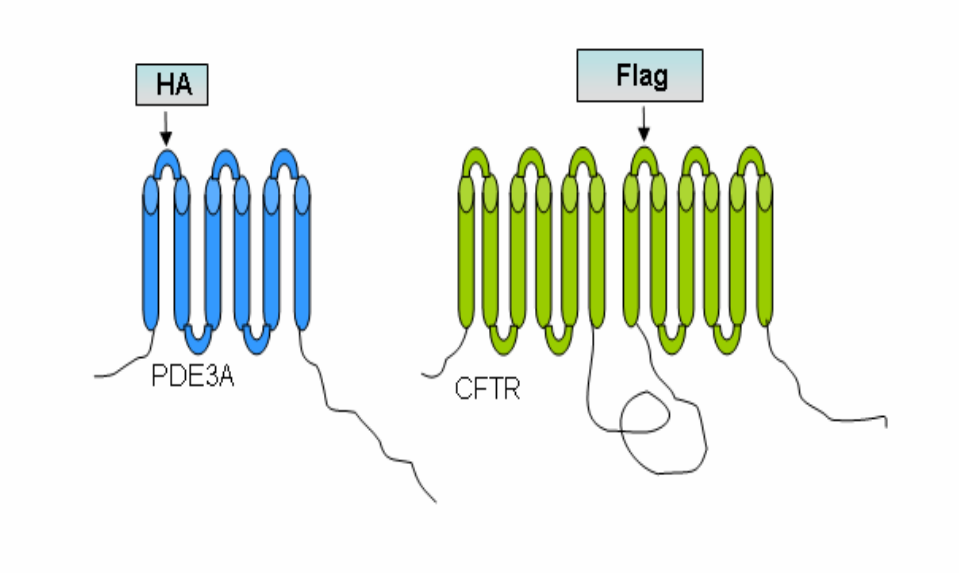

Figure 3-11. Generation of HA and Flag tagged PDE3A and CFTR

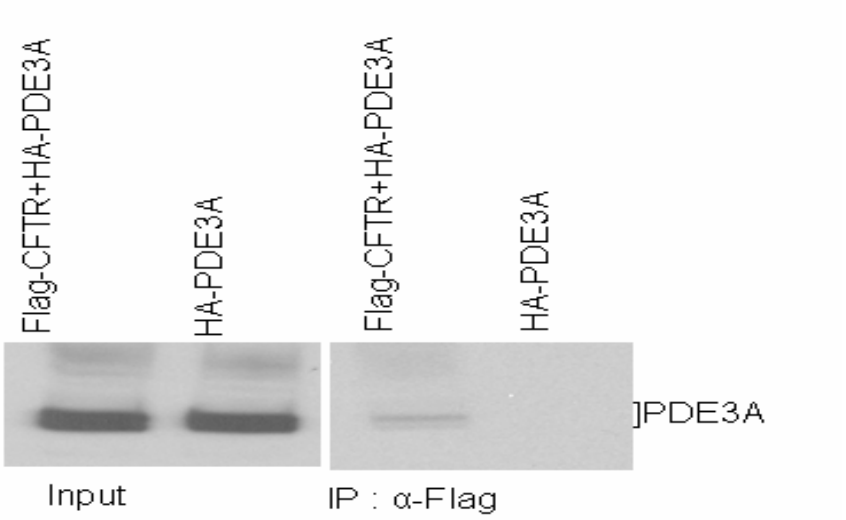

Figure 3-12. Co-immunoprecipitation shows interaction between PDE3A and CFTR

To investigate if the interaction between PDE3A and CFTR is direct, we purified full-length Flag-CFTR and full-length biotinylated HA-PDE3A. Amplified luminescent proximity homogeneous assay (AlphaScreen^{TM}) FLAG (M2) detection kit was used to study the interaction between these two purified proteins. A schematic diagram for alphascreen assay is shown in Fig. 3-13. The AlphaScreen^{TM} assay is a highly sensitive method which can be used to detect direct interactions between interacting partners at femtomolar concentrations (Ullman et al., 1996). For these studies, we kept Flag-CFTR concentration constant (100 nM final concentration) and used increasing concentrations of biotinylated HA-PDE3A (10 pM to 100 nM). As can be seen from Fig. 3-14, HA-PDE3A interacts directly with Flag-CFTR at nanomolar concentrations and in a dose-dependent manner.

To test whether the increased interaction between PDE3A and CFTR by PKA phosphorylation is due to the altered surface expression levels of PDE3A, we used surface labeling assay to study the expression of Flag- or HA-PDE3A at the plasma membrane of Calu-3 cells. A schematic diagram for surface labeling assay is shown in Fig. 3-15. Calu-3 cells endogenously expressing PDE3A were used as control. The formaldehyde-fixed cells were labeled with α-Flag-HRP or α-HA-HRP and incubated with HRP substrate 1-step Ultra TMB. The reaction was stopped by addition of 2 M H_2SO_4 and absorbance was read at 450 nm. As shown in Fig. 3-16, Flag- or HA-PDE3A is expressed at the plasma membrane of Calu-3 cells and the tags are indeed on the outer loop of the protein.

To further verify the surface expression of PDE3A, we surface labeled HEK293 cells expressing HA-PDE3A with a cell-impermeable biotinylating reagent Sulfo-NHS-LC-biotin at 4°C, lysed the cells and immunoprecipitated using α-HA agarose beads. The purified biotinylated HA-PDE3A was pulled down using streptavidin beads and the bound and unbound fractions were immunoblotted for PDE3A. HEK293 parental cells were used as negative control. We found that more than 90% of PDE3A is present at the plasma membrane of transfected HEK293 cells (Fig. 3-17). Next, we investigated the effects of PKA-phosphorylation on the surface expression levels of Flag-PDE3A. Calu-3 cells transfected with Flag-PDE3A were pre-treated with PKA activating agonist (forskolin, 20 μM) and then subjected to surface labeling as described above. The results showed that PKA-phosphorylation does not increase PDE3A surface expression levels as indicated by the unchanged absorbance between forskolin pre-treated cells and untreated cells (Fig. 3-18).

Based on these results, we proposed that, PDE3A and CFTR are in close proximity to each other at the plasma membrane of epithelial cells (e.g., Calu-3 cells). Inhibition of PDE3A generates highly compartmentalized cAMP, which further clusters PDE3A and CFTR into microdomains and augments CFTR channel function in a compartmentalized manner.

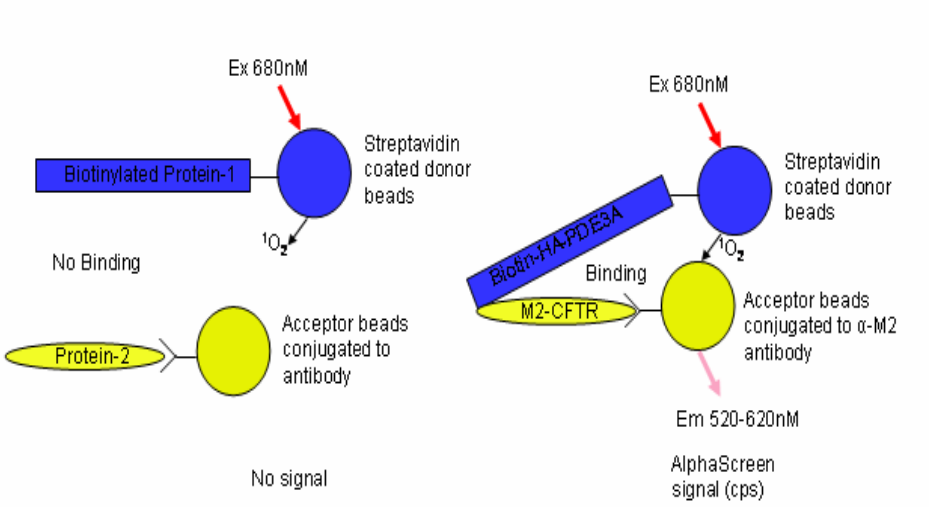

Figure 3-13. Schematic diagram for alphascreen assay

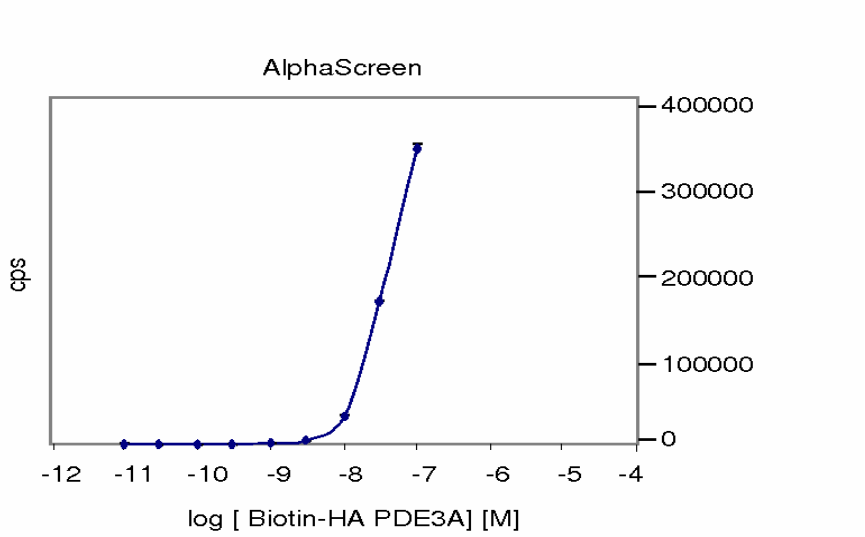

Figure 3-14. AlphaScreen™ indicates direct interaction of purified CFTR and PDE3A

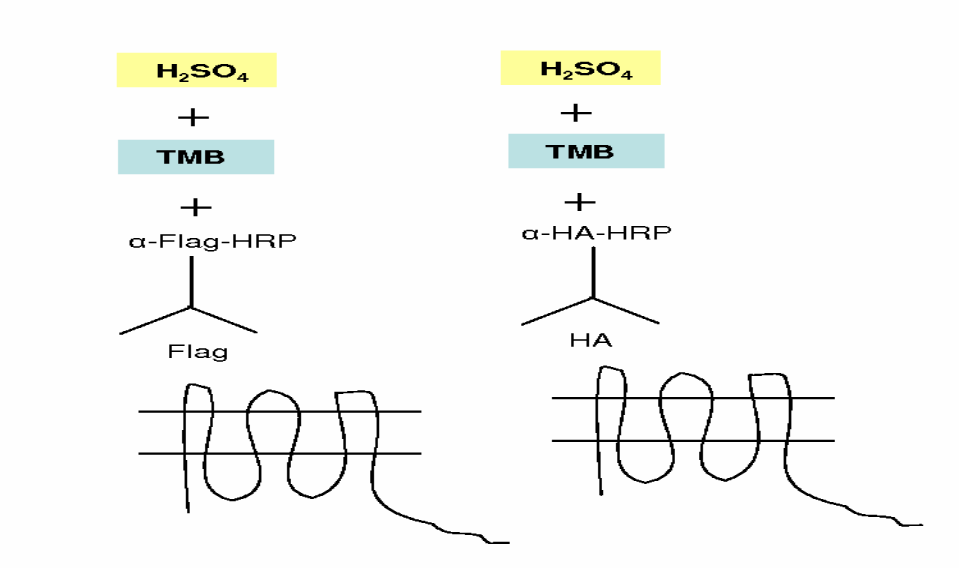

Figure 3-15. Schematic diagram for surface labeling assay

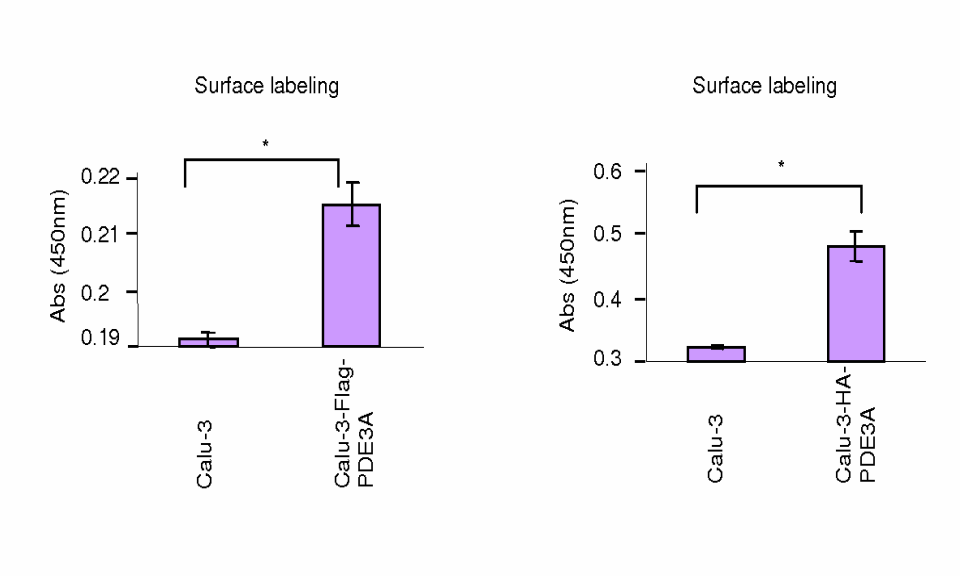

Figure 3-16. Flag and HA tagged PDE3A are expressed on the plasma membrane

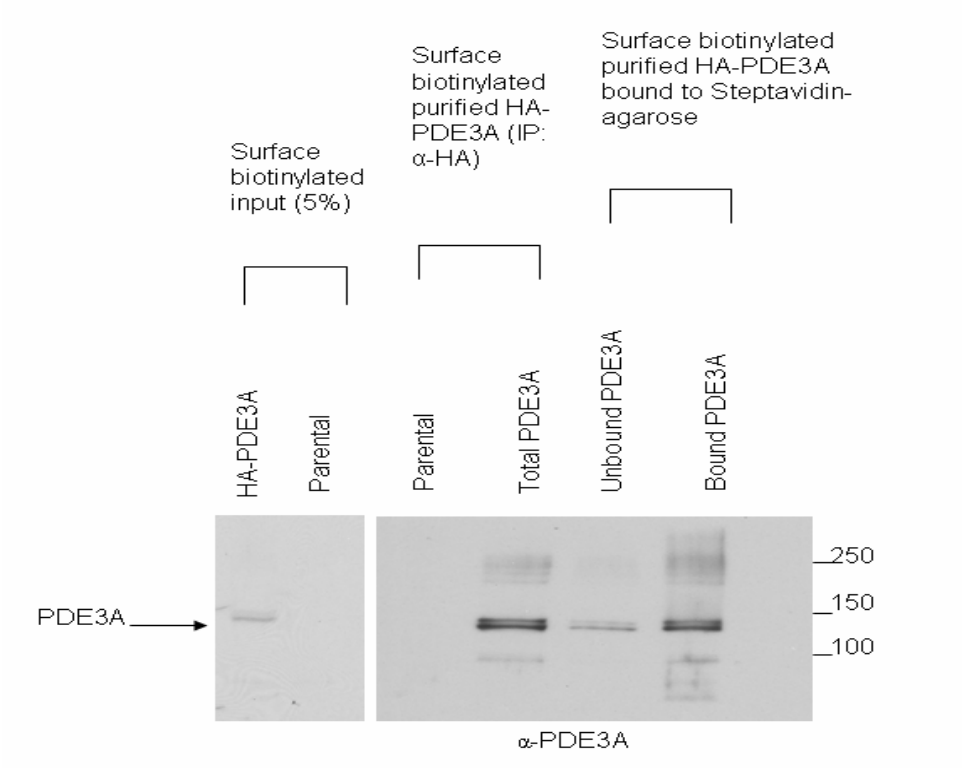

Figure 3-17. The majority of PDE3A is expressed on the membrane

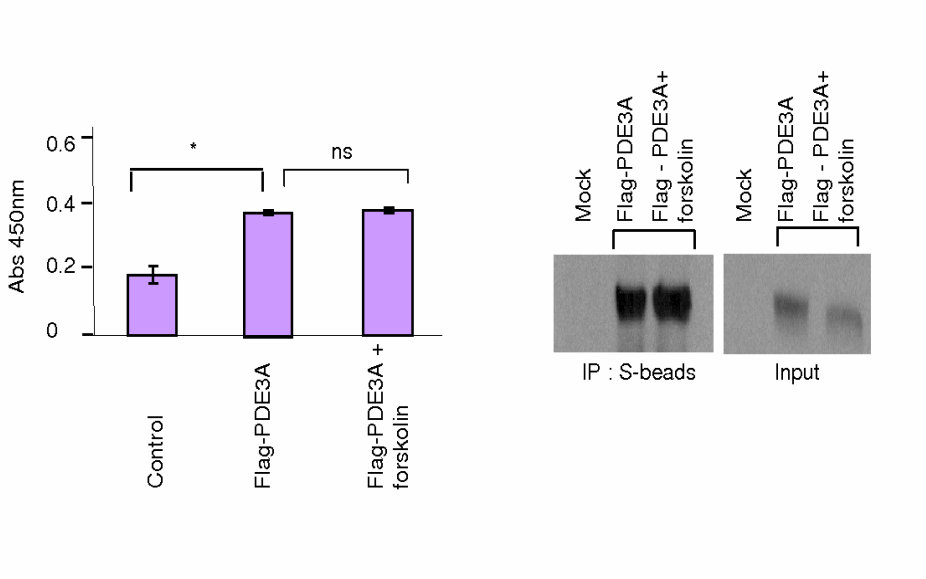

Figure 3-18. PKA phosphorylation does not alter surface expression of PDE3A

Cytoskeleton disruption reduces the physical and functional interaction between PDE3A and CFTR

All of the described data suggested the physical and functional coupling between PDE3A and CFTR. The next question we asked was: can we dissociate the clusters of PDE3A and CFTR at the plasma membrane and would this dissociation alter specifically PDE3A-dependent CFTR Cl^- channel function? Actin cytoskeleton has been shown to be important for maintaining CFTR in highly restricted domains on the plasma membrane (Jin et al., 2007). Actin filament organization has also been shown to play functional role in the activation and regulation of CFTR Cl^- channel function (Cantiello, 1996; Chasan et al., 2002; Ganeshan et al., 2007). Therefore, we continued to investigate the effects of cytoskeleton disruption on the physical and functional coupling between PDE3A and CFTR to see if cytoskeleton plays an important role in the physical and functional integrity of macromolecular complexes. Latrunculin B, a specific actin-disrupting reagent which causes actin filament depolymerization, was used for these purposes.

We first investigated the effects of actin cytoskeleton disruption on HA-PDE3A dynamics in live Calu-3 cells by using single particle tracking (SPT) method. A schematic diagram of single particle tracking assay is shown in Fig. 3-19. SPT is a powerful method to study the dynamics of individual proteins in the plasma membrane of live cells (Chen et al., 2006). HA-PDE3A (HA tag on the first outer loop at position 104) was labeled with biotin α-HA antibody and then conjugated to streptavidin-conjugated Qdot-655 for monitoring lateral mobility on the plasma membrane. The mean diffusion coefficient of PDE3A (0.0025 $\mu m^2/s$) we observed in this study is similar to that reported for CFTR (Bates et al., 2006; Jin et al., 2007), indicating the confined diffusion of PDE3A. As shown in Fig. 3-20, when the cells were treated with latrunculin B (1 μM), a significant increase in the mean squared displacement (MSD) and diffusion coefficient of PDE3A was observed (mean diffusion coefficient: 0.0117 $\mu m^2/s$; a 4.7-fold increase compared to the untreated cells). It is reasonable to propose that actin cytoskeleton disruption compromised the integrity of multiprotein complex and caused PDE3A to move freely, thus uncoupling PDE3A from the CFTR-containing complex.

To further investigate if the physical interaction between PDE3A and CFTR was reduced with cytoskeleton disruption, we co-transfected HEK293 cells with Flag-CFTR and HA-PDE3A and cross-linked these two proteins in live cells using dithiobissuccinimidyl propionate (DSP; 1 mM) with or without latrunculin B treatment. The cells were then lysed in RIPA buffer (containing 1 M urea) to disrupt all interactions except antigen-antibody interaction and the proteins were co-immunoprecipitated using α-HA beads and immunoblotted for CFTR. HEK 293 cells expressing only Flag-CFTR were used as negative control. DSP is a thiol-cleavable, amine-reactive homobifunctional cross-linker which has been used to cross-link proteins of interest in live cells (Li et al., 2004). The result showed that latrunculin B treatment led to a significant decrease in PDE3A-CFTR interaction (Fig. 3-21).

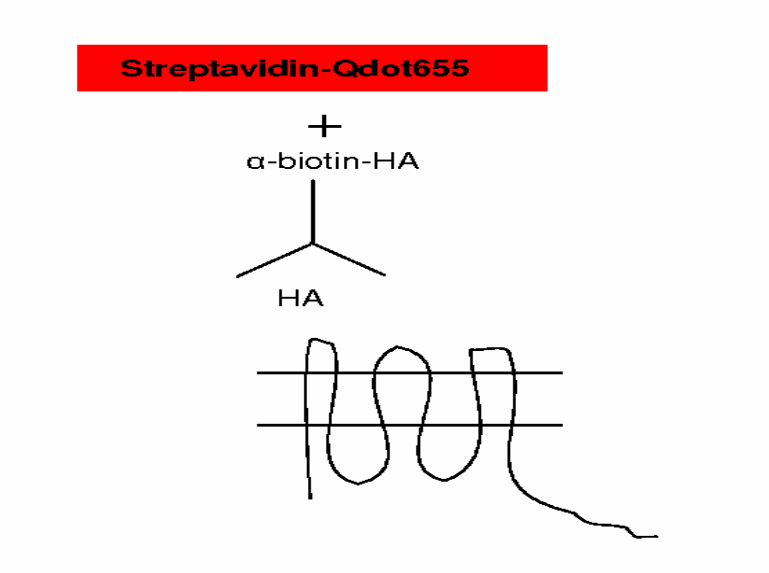

Figure 3-19. Schematic diagram of single particle tracking assay

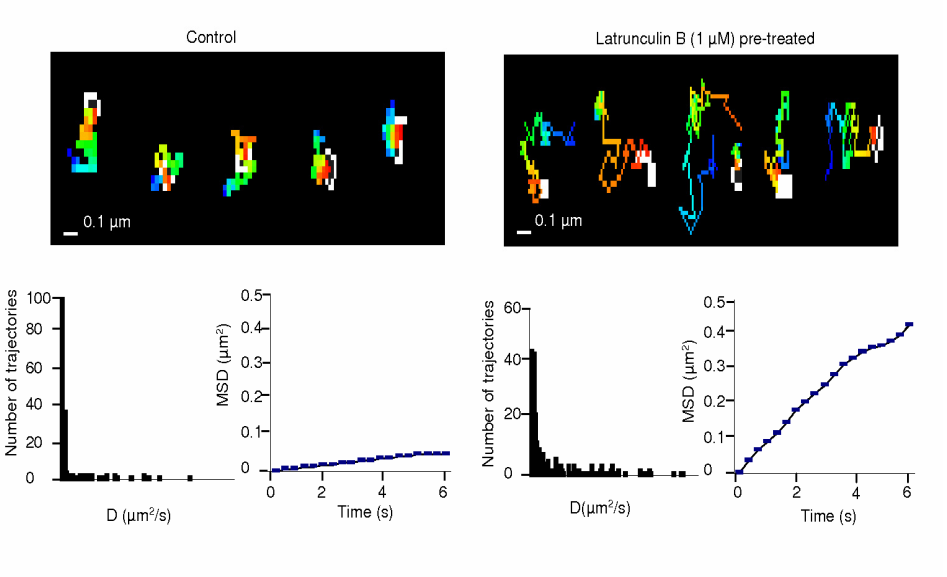

Figure 3-20. Single particle tracking of PDE3A with or without latrunculin B shows different diffusion patterns

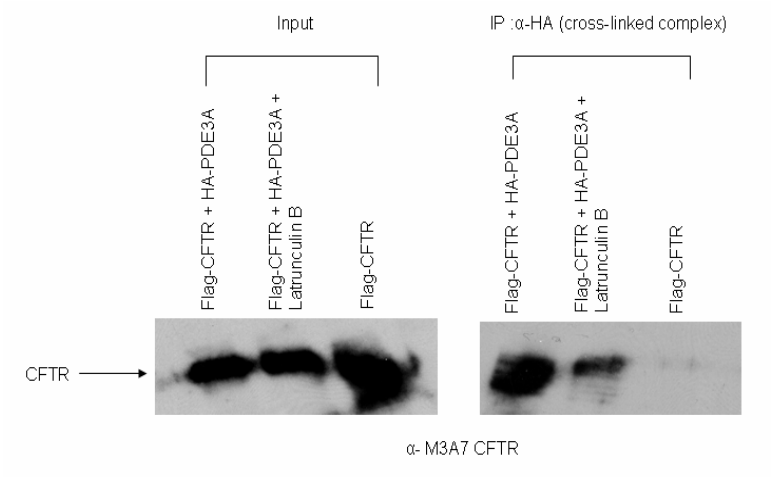

Figure 3-21. Latrunculin B decreases physical interaction between CFTR and PDE3A

We also tested the effects of actin disruption on functional coupling between PDE3A and CFTR. To test our hypothesis in a physiologically relevant system, we used latrunculin B in pig trachea submucosal gland secretion studies. As can be seen in Fig. 3-22, when treated with latrunculin B, a significant decrease (> 90%) in cilostazol-activated and CFTR-dependent mean mucosal secretion was observed. The data are consistent with the findings from the I_{SC} studies. We observed that latrunculin B itself can cause a small decrease of mean mucosal secretion rate. We ruled out the possibility of altered surface expression of PDE3A on latrunculin B treatment by using surface labeling assay which showed that the surface expression level of PDE3A is not significantly changed (Fig. 3-23).

CFTR-dependent short-circuit currents were measured in polarized Calu-3 cells mounted in an Ussing chamber. As shown in Fig. 3-24, I_{SC} measurements in cells treated with latrunculin B showed that the potentiating effects of PDE3A inhibition (cilostazol: 10-100 μM) on CFTR-dependent currents decreased by almost 65-80% compared to the cells without latrunculin B treatment. However, it is to be noted that the maximally-stimulated I_{SC} by forskolin (by increasing global cAMP) remained unaffected by latrunculin B treatment (Fig. 3-24).

Cell-attached single-channel recording in Calu-3 cells strongly supported our hypothesis and shed more mechanistic insights into the physical and functional coupling between PDE3A and CFTR and its actin cytoskeleton dependence. Cilostazol or forskolin was applied in the pipette to active CFTR channel function. As shown in Fig. 3-25, there was no significant change in single channel conductance for cells activated by either cilostazol or forskolin with or without latrunculin B treatment. CFTR channel open probability was significantly decreased in cilostazol activated currents when treated with latrunculin B. However, forskolin activated currents were not altered with latrunculin B treatment.

These data clearly indicated that PDE3A inhibition activated CFTR channel function in a compartmentalized manner and the coupling between these two proteins was actin cytoskeleton dependent. Cumulatively, our findings provided clear evidence that, 1) PDE3A was physically, and functionally, coupled to CFTR at the plasma membrane through compartmentalized cAMP; 2) inhibition of PDE3A generated high levels of compartmentalized cAMP which further clustered the two proteins into microdomains and potentiated CFTR Cl^- channel function; 3) cytoskeleton disruption decreased CFTR-PDE3A interaction, probably by scattering CFTR and PDE3A away from each other and compromising the integrity of the macromolecular signaling complexes, leading to the loss of compartmentalized cAMP signaling. Consequently, inhibition of PDE3A no longer potentiated CFTR Cl^- channel function in compartmentalized fashion. A model for CFTR and PDE3A coupling via compartmentalized cAMP generation is shown in Fig. 3-26.

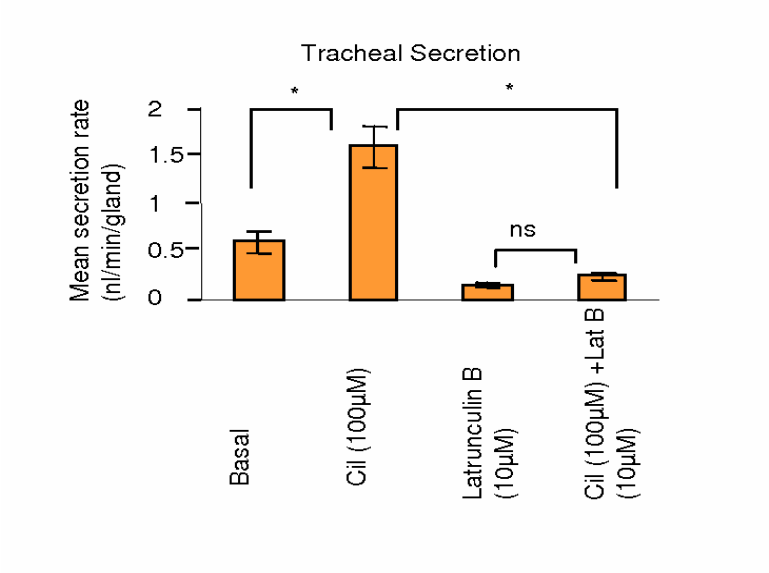

Figure 3-22. CFTR dependent tracheal submucosal gland secretion is not increased with PDE3 inhibition when treated with latrunculin B

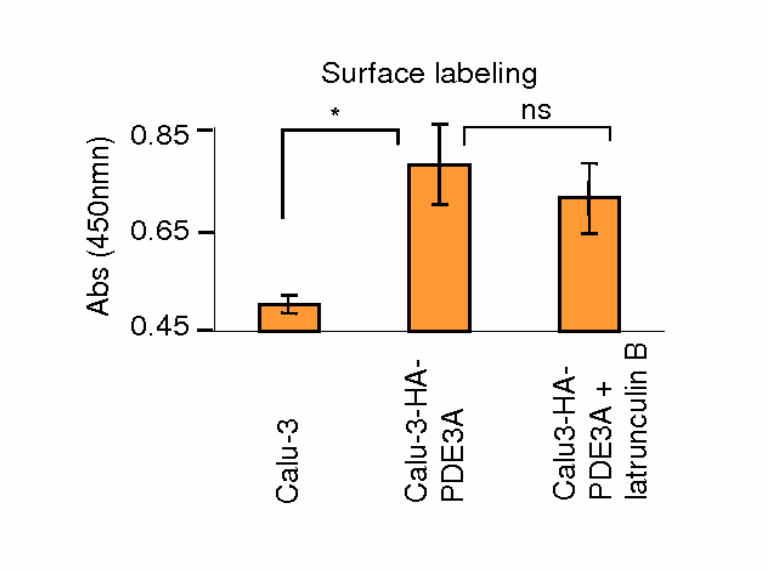

Figure 3-23. Surface expression of PDE3A is not altered in the presence of latrunculin B

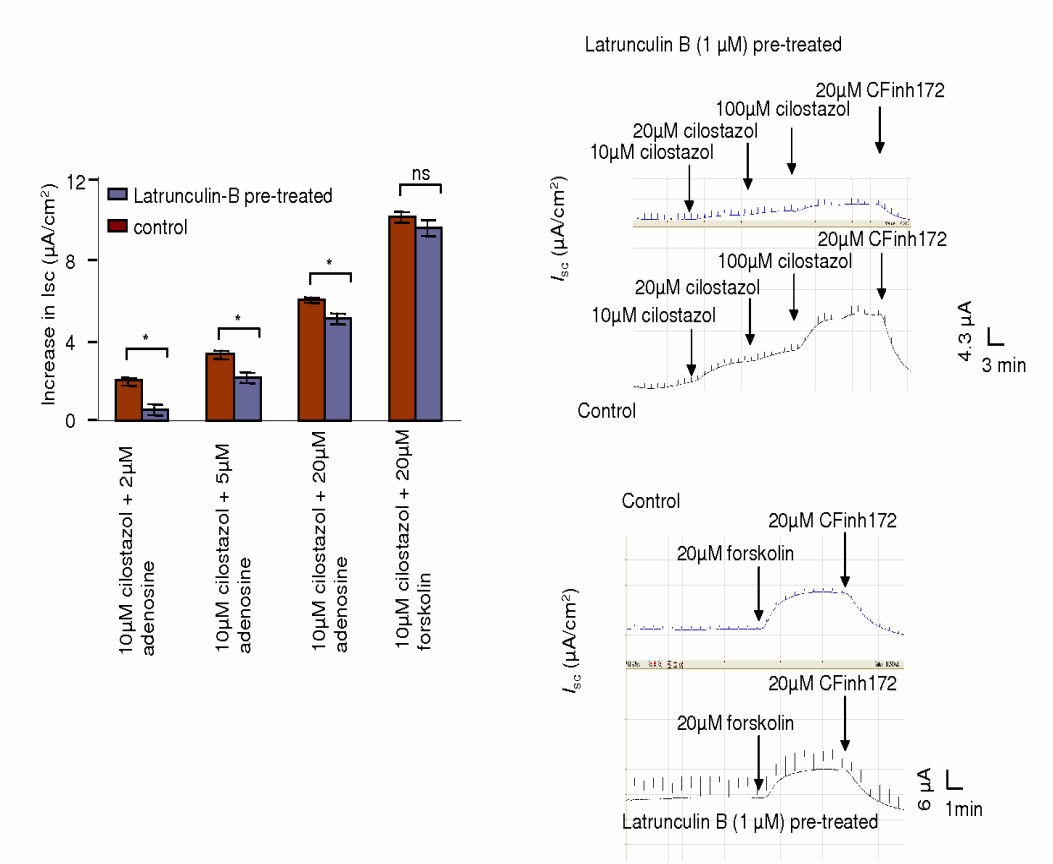

Figure 3-24. Latrunculin treatment inhibits local increase of CFTR function by PDE3 inhibition whereas global increase by forskolin is not altered

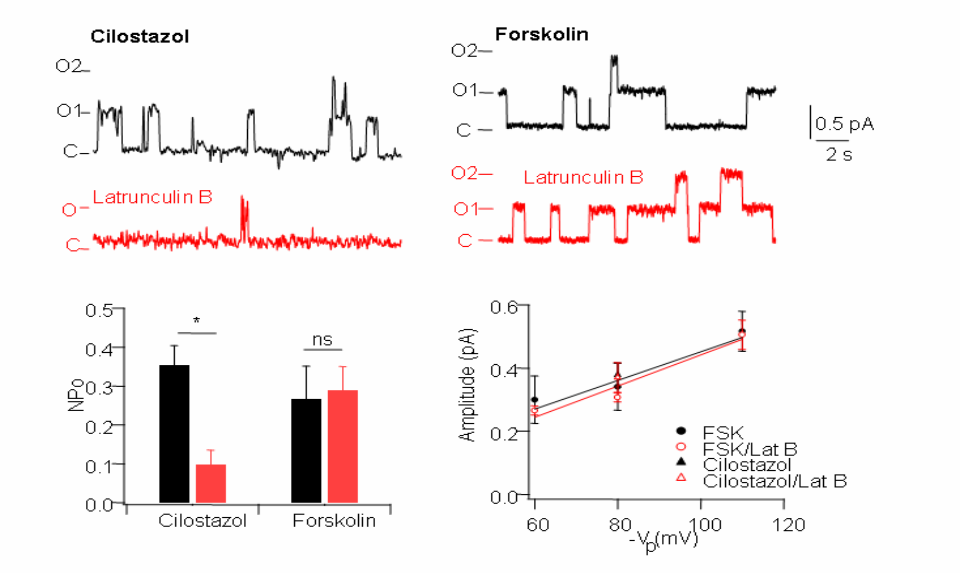

Figure 3-25. Latrunculin B treatment alters open probablility of CFTR with PDE3 inhibition whereas forskolin response is unaltered

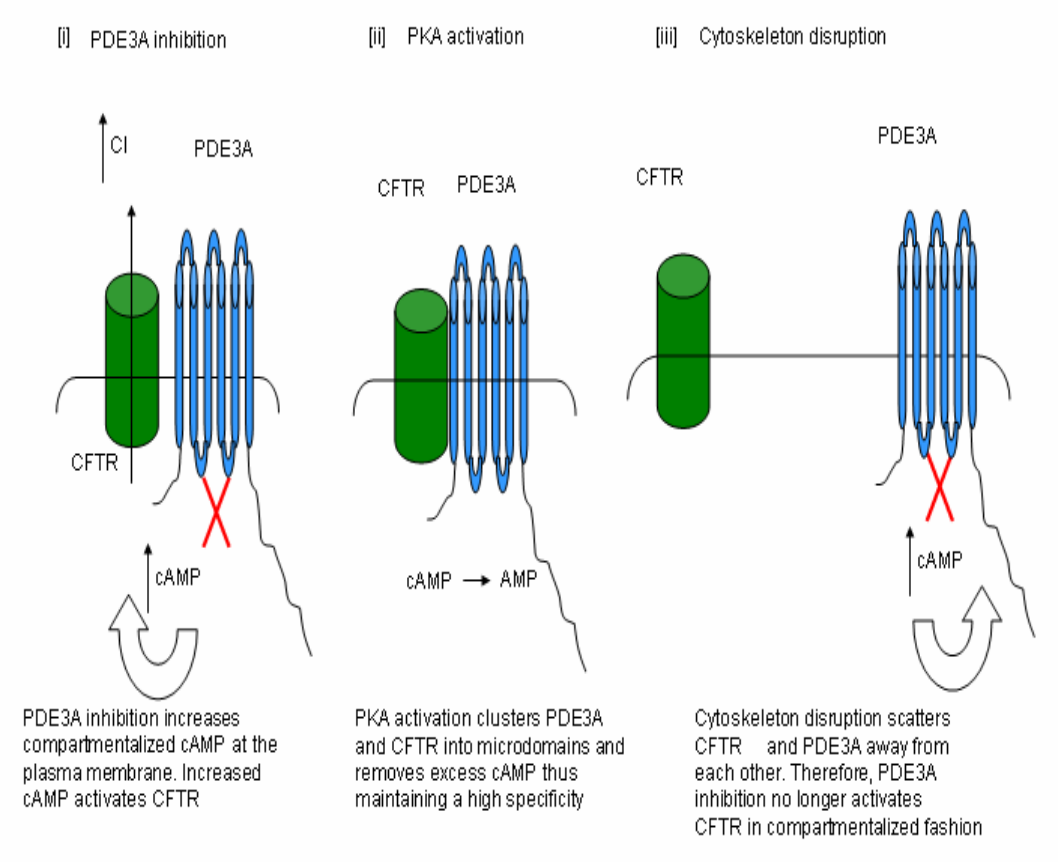

Figure 3-26. Model for PDE3A and CFTR coupling via compartmentalized cAMP

CHAPTER 4: DISCUSSION

It is now well accepted that the formation of multiple-protein macromolecular complexes at specialized subcellular microdomains increases the specificity and efficiency of signaling in cells (Li & Naren, 2005; Li et al., 2007). The main goal of this study was to investigate the physical and functional coupling between CFTR Cl^- channel and PDE3A and its physiological relevance in airway gland mucus secretion.

Physical and Functional Coupling between CFTR and PDE3A

In this study, we found that PDE3A is expressed at the plasma membrane of epithelial cells of pig trachea, Calu-3 cells, and HEK293 cells. These data are supported by results from immunohistochemical analysis, Western blotting and cell surface labeling studies. We demonstrated that CFTR directly interacts with PDE3A in a PKA-dependent manner by using FRET, cross-linking, co-immunoprecipitation and AlphaScreen^{TM} assay. We also observed the functional coupling between PDE3A and CFTR Cl^- channel function. Inhibition of PDE3A augmented CFTR Cl^- channel function as seen in I_{SC} and iodide efflux measurements. Studies on cAMP localization and dynamics by using a FRET-based cAMP sensor, CFP-EPAC-YFP, showed that, upon PDE3A inhibition, cAMP was generated in highly compartmentalized fashion at the plasma membrane. All these data indicated that CFTR and PDE3A form macromolecular complexes at the plasma membrane through compartmentalized cAMP. This hypothesis was further supported by the facts that actin cytoskeleton disruption decreased CFTR-PDE3A interaction, probably by scattering CFTR and PDE3A away from each other and compromising the integrity of the macromolecular complexes. Consequently, inhibition of PDE3A no longer activated CFTR Cl^- channel function in compartmentalized fashion as evidenced by cell-attached single-channel recording studies, I_{SC} measurements and pig tracheal submucosal gland secretion studies in the presence of latrunculin B, an actin skeleton disrupting reagent. Based on these results, we propose a model to depict the mechanism through which the physical and functional coupling between PDE3A and CFTR Cl^- channel occurs.

Compartmentalized cAMP and PDE3A Signaling

One of the key features of cAMP/PKA signal transduction system has been suggested to be the compartmentalization of its signaling enzymes and effectors that generates localized cAMP and activates PKA at distinct subcellular locations (Zaccolo, 2006). PDEs have been shown to play vital roles in such compartmentalized signaling processes. The emerging idea is that it is the compartmentalization of individual PDEs, rather than total expression level, which is of vital importance in modulating localized intracellular cAMP levels (Zaccolo, 2006). Kinase-anchoring proteins (AKAPs) have been reported to play key roles in the assembly and organization of such compartmentalized cAMP/PKA signaling. AKAPs anchor PKA and PDEs to specific

intracellular locations in close vicinity to specific modulators and targets to achieve signaling specificity and efficiency (Langeberg & Scott, 2005; McConnachie et al., 2006). Tasken et al. reported that PDE4D3 and PKA form a signaling complex in the centrosomal area which is coordinated by the centrosomal AKAP450 and regulates accurate spatiotemporal cAMP signals (Tasken et al., 2001). Lee et al. demonstrated that a PDZ-containing protein, Shank2, competes with NHERF1 for binding to CFTR. Shank2 associates with PDE4D and tethers it to CFTR complex and thus attenuates cAMP/PKA signals (Lee et al., 2007). Pozuelo et al. reported that PDE3A binds directly to 14-3-3 proteins in a phosphorylation-dependent manner and PDE3A also binds to plectin, a cytoskeletal linker protein (Pozuelo Rubio et al., 2005). More recently, Puxeddu et al. demonstrated that PDE3A interacts with brefeldin A-inhibited guanine nucleotide-exchange proteins (BIG1 and BIG2) in HeLa cell cytosol via compartmentalized cAMP signaling with spatial and temporal specificity (Puxeddu et al., 2009).

In this study, we report a previously unknown physical and functional coupling between CFTR and PDE3A and propose that they form a signaling macromolecular complex at the plasma membrane. Other signaling components such as specific G protein-coupled receptors (GPCRs), G proteins (G_s), AC, PKA and anchoring proteins (AKAPs) may also be present in the proposed macromolecular complexes which synergistically regulate compartmentalized cAMP signaling and specificity of CFTR activation.

Physiological Relevance of CFTR-PDE3A-containing Macromolecular Complexes in Airway Gland Mucus Secretion

Regulation of CFTR channel function via its interaction with PDE3A is of physiological and pathophysiological importance owing to: 1) CFTR is the primary cAMP-activated Cl^- channel on the apical membrane of airway epithelia, thus playing critical roles in controlling the electrolyte/fluid balance and mucociliary clearance process (Pilewski & Frizzell, 1999), 2) phosphodiesterase inhibition remains a viable area of therapy for the treatment of airway diseases such as asthma and COPD (Fan Chung, 2006). Submucosal gland secretion has been reported to play important roles in maintaining airway and lung health and CFTR has been shown to play important roles in such process. This idea is supported by the observations that CF glands have altered response to secretagogues compared with normal glands (Ianowski et al., 2008) and by the fact that in CF patients the airway host defenses system are compromised, leading to chronic secondary bacterial infections and inflammation in the lung and respiratory failure (Pilewski & Frizzell, 1999; Sheppard & Welsh, 1999).

Drugs targeting PDEs are being considered for their cardiotonic, pulmonary vasodilator, smooth muscle relaxant, antithrombotic, antiinflammtory, and antiasthmatic properties (Conti & Beavo, 2007). Targeted inhibition of PDE4 has been pursued as a way of reducing inflammation in patients with asthma or COPD, diseases characterized by mucus-congested and inflamed airways (Barnette, 1999; Compton et al., 2001).

Cilomilast and roflumilast, two second generation PDE4 inhibitors, have shown potential benefit for treatment of asthma and COPD. However, clinical utility of PDE4 inhibitors has been limited by adverse effects, including nausea, diarrhea, and vomiting (Fan Chung, 2006; Halpin, 2008).

Although PDE3 inhibitors do not appear to have direct anti-inflammatory actions, they have been shown to augment the anti-inflammatory actions of PDE4 inhibitors (Giembycz et al., 1996; Schudt et al., 1995). Also, PDE3 inhibitors could act as bronchodilators and may have synergistic effects with PDE4 inhibitors (Halpin, 2008). Development of dual specificity inhibitors (such as dual PDE3-PDE4 inhibitors) may provide more bronchodilator and bronchoprotective effect in addition to the beneficial PDE4 effects (Giembycz, 2005).

PDE3 and PDE4 have been reported to be the major PDEs present in airway epithelial cells (Torphy, 1998; Wright et al., 1998). Inhibition of PDE4 and/or PDE3 has been demonstrated to activate CFTR Cl^- channel function (Cobb et al., 2003; Kelley et al., 1995; Liu et al., 2005). However, the mechanism through which the functional coupling occurs remains unclear. In this study, we demonstrated that PDE3A is physically and functionally coupled to CFTR and form macromolecular complexes together with other signaling molecules. Inhibition of PDE3A augments CFTR Cl^- channel function by generation of highly compartmentalized cAMP. However, inhibition of PDE4 using rolipram led to globally increased cAMP. These findings not only provide insights into the important roles of PDE3A in compartmentalized cAMP signaling processes, but may also have important implications in the therapeutic interventions of diseases such as CF, asthma, and COPD: 1) targeting PDE3A and development of isoform-specific PDE3A inhibitors (or dual specificity inhibitors) may open new avenue in PDEs drug development, 2) inhibition of PDE3A has the beneficial effects of localized potentiation of CFTR channel function (through compartmentalized signaling) and thus submucosal gland secretion. These additional benefits would help to restore and maintain airway and lung health.

In this study, we have identified that compartmentalized cAMP at the plasma membrane is generated by inhibiting PDE3A, which is functionally and physically coupled to the CFTR chloride channel and thus to tracheal mucosal secretion. We suggest that PDE3A and CFTR are in close proximity to each other on the plasma membrane. Inhibition of PDE3A lead to generation of compartmentalized cAMP at the plasma membrane, which, in turn, lead to increased clustering of these two proteins and the maintenance of a high degree of specificity. Actin cytoskeleton disruption altered PDE3A dynamics and its physical and functional coupling with CFTR. Such regulation of CFTR function via its interaction with PDE3A might be of physiological relevance owing to the relevance of CFTR in fluid transport and homeostasis.

LIST OF REFERENCES

Abraham, G., Kottke, C., Dhein, S. & Ungemach, F. R. (2003). Pharmacological and biochemical characterization of the beta-adrenergic signal transduction pathway in different segments of the respiratory tract. Biochem Pharmacol. 66, 1067-81.

Amaral, M. D. & Kunzelmann, K. (2007). Molecular targeting of CFTR as a therapeutic approach to cystic fibrosis. Trends Pharmacol Sci. 28, 334-41.

Anderson, M. P., Berger, H. A., Rich, D. P., Gregory, R. J., Smith, A. E. & Welsh, M. J. (1991). Nucleoside triphosphates are required to open the CFTR chloride channel. Cell. 67, 775-84.

Ballard, S. T. & Spadafora, D. (2007). Fluid secretion by submucosal glands of the tracheobronchial airways. Respir Physiol Neurobiol. 159, 271-7.

Barnes, P. J. (1996). Pathophysiology of asthma. Br J Clin Pharmacol. 42, 3-10.

Barnette, M. S. (1999). Phosphodiesterase 4 (PDE4) inhibitors in asthma and chronic obstructive pulmonary disease (COPD). Prog Drug Res. 53, 193-229.

Basbaum, C. B., Jany, B. & Finkbeiner, W. E. (1990). The serous cell. Annu Rev Physiol. 52, 97-113.

Bates, I. R., Hebert, B., Luo, Y., Liao, J., Bachir, A. I., Kolin, D. L., Wiseman, P. W. & Hanrahan, J. W. (2006). Membrane lateral diffusion and capture of CFTR within transient confinement zones. Biophys J. 91, 1046-58.

Bear, C. E., Li, C. H., Kartner, N., Bridges, R. J., Jensen, T. J., Ramjeesingh, M. & Riordan, J. R. (1992). Purification and functional reconstitution of the cystic fibrosis transmembrane conductance regulator (CFTR). Cell. 68, 809-18.

Beavo, J. A. (1995). Cyclic nucleotide phosphodiesterases: functional implications of multiple isoforms. Physiol Rev. 75, 725-48.

Benharouga, M., Haardt, M., Kartner, N. & Lukacs, G. L. (2001). COOH-terminal truncations promote proteasome-dependent degradation of mature cystic fibrosis transmembrane conductance regulator from post-Golgi compartments. J Cell Biol. 153, 957-70.

Bolger, G. B., Peden, A. H., Steele, M. R., MacKenzie, C., McEwan, D. G., Wallace, D. A., Huston, E., Baillie, G. S. & Houslay, M. D. (2003). Attenuation of the activity of the cAMP-specific phosphodiesterase PDE4A5 by interaction with the immunophilin XAP2. J Biol Chem. 278, 33351-63.

Cantiello, H. F. (1996). Role of the actin cytoskeleton in the regulation of the cystic fibrosis transmembrane conductance regulator. Exp Physiol. 81, 505-14.

Cantiello, H. F. (2001). Role of actin filament organization in CFTR activation. Pflugers Arch. 443 Suppl 1, S75-80.

Cantiello, H. F., Prat, A. G., Bonventre, J. V., Cunningham, C. C., Hartwig, J. H. & Ausiello, D. A. (1993). Actin-binding protein contributes to cell volume regulatory ion channel activation in melanoma cells. J Biol Chem. 268, 4596-9.

Cantiello, H. F., Stow, J. L., Prat, A. G. & Ausiello, D. A. (1991). Actin filaments regulate epithelial Na+ channel activity. Am J Physiol. 261, C882-8.

Chasan, B., Geisse, N. A., Pedatella, K., Wooster, D. G., Teintze, M., Carattino, M. D., Goldmann, W. H. & Cantiello, H. F. (2002). Evidence for direct interaction between actin and the cystic fibrosis transmembrane conductance regulator. Eur Biophys J. 30, 617-24.

Chen, Y., Lagerholm, B. C., Yang, B. & Jacobson, K. (2006). Methods to measure the lateral diffusion of membrane lipids and proteins. Methods. 39, 147-53.

Cheng, J., Moyer, B. D., Milewski, M., Loffing, J., Ikeda, M., Mickle, J. E., Cutting, G. R., Li, M., Stanton, B. A. & Guggino, W. B. (2002). A Golgi-associated PDZ domain protein modulates cystic fibrosis transmembrane regulator plasma membrane expression. J Biol Chem. 277, 3520-9.

Choi, J. Y., Joo, N. S., Krouse, M. E., Wu, J. V., Robbins, R. C., Ianowski, J. P., Hanrahan, J. W. & Wine, J. J. (2007). Synergistic airway gland mucus secretion in response to vasoactive intestinal peptide and carbachol is lost in cystic fibrosis. J Clin Invest. 117, 3118-27.

Cobb, B. R., Fan, L., Kovacs, T. E., Sorscher, E. J. & Clancy, J. P. (2003). Adenosine receptors and phosphodiesterase inhibitors stimulate Cl- secretion in Calu-3 cells. Am J Respir Cell Mol Biol. 29, 410-8.

Compton, C. H., Gubb, J., Nieman, R., Edelson, J., Amit, O., Bakst, A., Ayres, J. G., Creemers, J. P., Schultze-Werninghaus, G., Brambilla, C. & Barnes, N. C. (2001). Cilomilast, a selective phosphodiesterase-4 inhibitor for treatment of patients with chronic obstructive pulmonary disease: a randomised, dose-ranging study. Lancet. 358, 265-70.

Conti, M. & Beavo, J. (2007). Biochemistry and physiology of cyclic nucleotide phosphodiesterases: essential components in cyclic nucleotide signaling. Annu Rev Biochem. 76, 481-511.

Conti, M., Iona, S., Cuomo, M., Swinnen, J. V., Odeh, J. & Svoboda, M. E. (1995). Characterization of a hormone-inducible, high affinity adenosine 3'-5'-cyclic monophosphate phosphodiesterase from the rat Sertoli cell. Biochemistry. 34, 7979-87.

Cooper, D. M. (2005). Compartmentalization of adenylate cyclase and cAMP signalling. Biochem Soc Trans. 33, 1319-22.

Degerman, E., Belfrage, P. & Manganiello, V. C. (1997). Structure, localization, and regulation of cGMP-inhibited phosphodiesterase (PDE3). J Biol Chem. 272, 6823-6.

Dodge, K. L., Khouangsathiene, S., Kapiloff, M. S., Mouton, R., Hill, E. V., Houslay, M. D., Langeberg, L. K. & Scott, J. D. (2001). mAKAP assembles a protein kinase A/PDE4 phosphodiesterase cAMP signaling module. Embo J. 20, 1921-30.

Dodge-Kafka, K. L., Langeberg, L. & Scott, J. D. (2006). Compartmentation of cyclic nucleotide signaling in the heart: the role of A-kinase anchoring proteins. Circ Res. 98, 993-1001.

Dunnill, M. S., Massarella, G. R. & Anderson, J. A. (1969). A comparison of the quantitative anatomy of the bronchi in normal subjects, in status asthmaticus, in chronic bronchitis, and in emphysema. Thorax. 24, 176-9.

Engelhardt, J. F., Yankaskas, J. R., Ernst, S. A., Yang, Y., Marino, C. R., Boucher, R. C., Cohn, J. A. & Wilson, J. M. (1992). Submucosal glands are the predominant site of CFTR expression in the human bronchus. Nat Genet. 2, 240-8.

Fahy, J. V., Schuster, A., Ueki, I., Boushey, H. A. & Nadel, J. A. (1992). Mucus hypersecretion in bronchiectasis. The role of neutrophil proteases. Am Rev Respir Dis. 146, 1430-3.

Fan Chung, K. (2006). Phosphodiesterase inhibitors in airways disease. Eur J Pharmacol. 533, 110-7.

Finkbeiner, W. E. (1999). Physiology and pathology of tracheobronchial glands. Respir Physiol. 118, 77-83.

Florio, S. K., Prusti, R. K. & Beavo, J. A. (1996). Solubilization of membrane-bound rod phosphodiesterase by the rod phosphodiesterase recombinant delta subunit. J Biol Chem. 271, 24036-47.

Galperin, E. & Sorkin, A. (2003). Visualization of Rab5 activity in living cells by FRET microscopy and influence of plasma-membrane-targeted Rab5 on clathrin-dependent endocytosis. J Cell Sci. 116, 4799-810.

Ganeshan, R., Nowotarski, K., Di, A., Nelson, D. J. & Kirk, K. L. (2007). CFTR surface expression and chloride currents are decreased by inhibitors of N-WASP and actin polymerization. Biochim Biophys Acta. 1773, 192-200.

Giembycz, M. A. (2005). Phosphodiesterase-4: selective and dual-specificity inhibitors for the therapy of chronic obstructive pulmonary disease. Proc Am Thorac Soc. 2, 326-33; discussion 340-1.

Giembycz, M. A., Corrigan, C. J., Seybold, J., Newton, R. & Barnes, P. J. (1996). Identification of cyclic AMP phosphodiesterases 3, 4 and 7 in human CD4+ and CD8+ T-lymphocytes: role in regulating proliferation and the biosynthesis of interleukin-2. Br J Pharmacol. 118, 1945-58.

Haardt, M., Benharouga, M., Lechardeur, D., Kartner, N. & Lukacs, G. L. (1999). C-terminal truncations destabilize the cystic fibrosis transmembrane conductance regulator without impairing its biogenesis. A novel class of mutation. J Biol Chem. 274, 21873-7.

Haggie, P. M., Kim, J. K., Lukacs, G. L. & Verkman, A. S. (2006). Tracking of quantum dot-labeled CFTR shows near immobilization by C-terminal PDZ interactions. Mol Biol Cell. 17, 4937-45.

Hall, R. A., Ostedgaard, L. S., Premont, R. T., Blitzer, J. T., Rahman, N., Welsh, M. J. & Lefkowitz, R. J. (1998). A C-terminal motif found in the beta2-adrenergic receptor, P2Y1 receptor and cystic fibrosis transmembrane conductance regulator determines binding to the Na+/H+ exchanger regulatory factor family of PDZ proteins. Proc Natl Acad Sci U S A. 95, 8496-501.

Halpin, D. M. (2008). ABCD of the phosphodiesterase family: interaction and differential activity in COPD. Int J Chron Obstruct Pulmon Dis. 3, 543-61.

Han, S. J., Vaccari, S., Nedachi, T., Andersen, C. B., Kovacina, K. S., Roth, R. A. & Conti, M. (2006). Protein kinase B/Akt phosphorylation of PDE3A and its role in mammalian oocyte maturation. Embo J. 25, 5716-25.

Huang, P., Lazarowski, E. R., Tarran, R., Milgram, S. L., Boucher, R. C. & Stutts, M. J. (2001). Compartmentalized autocrine signaling to cystic fibrosis transmembrane conductance regulator at the apical membrane of airway epithelial cells. Proc Natl Acad Sci U S A. 98, 14120-5.

Hunter, R. W., Mackintosh, C. & Hers, I. (2009). Protein kinase C-mediated phosphorylation and activation of PDE3A regulate cAMP levels in human platelets. J Biol Chem. 284, 12339-48.

Ianowski, J. P., Choi, J. Y., Wine, J. J. & Hanrahan, J. W. (2008). Substance P stimulates CFTR-dependent fluid secretion by mouse tracheal submucosal glands. Pflugers Arch. 457, 529-37.

Inglis, S. K., Corboz, M. R. & Ballard, S. T. (1998). Effect of anion secretion inhibitors on mucin content of airway submucosal gland ducts. Am J Physiol. 274, L762-6.

Jacquot, J., Puchelle, E., Hinnrasky, J., Fuchey, C., Bettinger, C., Spilmont, C., Bonnet, N., Dieterle, A., Dreyer, D., Pavirani, A. & et al. (1993). Localization of the cystic fibrosis transmembrane conductance regulator in airway secretory glands. Eur Respir J. 6, 169-76.

Jin, S., Haggie, P. M. & Verkman, A. S. (2007). Single-particle tracking of membrane protein diffusion in a potential: simulation, detection, and application to confined diffusion of CFTR Cl- channels. Biophys J. 93, 1079-88.

Joo, N. S., Wu, J. V., Krouse, M. E., Saenz, Y. & Wine, J. J. (2001). Optical method for quantifying rates of mucus secretion from single submucosal glands. Am J Physiol Lung Cell Mol Physiol. 281, L458-68.

Kelley, T. J., al-Nakkash, L. & Drumm, M. L. (1995). CFTR-mediated chloride permeability is regulated by type III phosphodiesterases in airway epithelial cells. Am J Respir Cell Mol Biol. 13, 657-64.

Langeberg, L. K. & Scott, J. D. (2005). A-kinase-anchoring proteins. J Cell Sci. 118, 3217-20.

Lee, J. H., Richter, W., Namkung, W., Kim, K. H., Kim, E., Conti, M. & Lee, M. G. (2007). Dynamic regulation of cystic fibrosis transmembrane conductance regulator by competitive interactions of molecular adaptors. J Biol Chem. 282, 10414-22.

Lehnart, S. E., Wehrens, X. H., Reiken, S., Warrier, S., Belevych, A. E., Harvey, R. D., Richter, W., Jin, S. L., Conti, M. & Marks, A. R. (2005). Phosphodiesterase 4D deficiency in the ryanodine-receptor complex promotes heart failure and arrhythmias. Cell. 123, 25-35.

Li, C., Dandridge, K. S., Di, A., Marrs, K. L., Harris, E. L., Roy, K., Jackson, J. S., Makarova, N. V., Fujiwara, Y., Farrar, P. L., Nelson, D. J., Tigyi, G. J. & Naren, A. P. (2005). Lysophosphatidic acid inhibits cholera toxin-induced secretory diarrhea through CFTR-dependent protein interactions. J Exp Med. 202, 975-86.

Li, C., Krishnamurthy, P. C., Penmatsa, H., Marrs, K. L., Wang, X. Q., Zaccolo, M., Jalink, K., Li, M., Nelson, D. J., Schuetz, J. D. & Naren, A. P. (2007). Spatiotemporal Coupling of cAMP Transporter to CFTR Chloride Channel Function in the Gut Epithelia. Cell. 131, 940-51.

Li, C. & Naren, A. P. (2005). Macromolecular complexes of cystic fibrosis transmembrane conductance regulator and its interacting partners. Pharmacol Ther. 108, 208-23.

Li, C., Roy, K., Dandridge, K. & Naren, A. P. (2004). Molecular assembly of cystic fibrosis transmembrane conductance regulator in plasma membrane. J Biol Chem. 279, 24673-84.

Liu, S., Veilleux, A., Zhang, L., Young, A., Kwok, E., Laliberte, F., Chung, C., Tota, M. R., Dube, D., Friesen, R. W. & Huang, Z. (2005). Dynamic activation of cystic fibrosis transmembrane conductance regulator by type 3 and type 4D phosphodiesterase inhibitors. J Pharmacol Exp Ther. 314, 846-54.

Liu, Y., Shakur, Y., Yoshitake, M. & Kambayashi Ji, J. (2001). Cilostazol (pletal): a dual inhibitor of cyclic nucleotide phosphodiesterase type 3 and adenosine uptake. Cardiovasc Drug Rev. 19, 369-86.

Manganiello, V. C., Taira, M., Degerman, E. & Belfrage, P. (1995). Type III cGMP-inhibited cyclic nucleotide phosphodiesterases (PDE3 gene family). Cell Signal. 7, 445-55.

Matthay, M. A., Folkesson, H. G. & Clerici, C. (2002). Lung epithelial fluid transport and the resolution of pulmonary edema. Physiol Rev. 82, 569-600.

Matthay, M. A., Robriquet, L. & Fang, X. (2005). Alveolar epithelium: role in lung fluid balance and acute lung injury. Proc Am Thorac Soc. 2, 206-13.

McConnachie, G., Langeberg, L. K. & Scott, J. D. (2006). AKAP signaling complexes: getting to the heart of the matter. Trends Mol Med. 12, 317-23.

Meacci, E., Taira, M., Moos, M., Jr., Smith, C. J., Movsesian, M. A., Degerman, E., Belfrage, P. & Manganiello, V. (1992). Molecular cloning and expression of human myocardial cGMP-inhibited cAMP phosphodiesterase. Proc Natl Acad Sci U S A. 89, 3721-5.

Meyrick, B. & Reid, L. (1970). Ultrastructure of cells in the human bronchial submucosal glands. J Anat. 107, 281-99.

Meyrick, B., Sturgess, J. M. & Reid, L. (1969). A reconstruction of the duct system and secretory tubules of the human bronchial submucosal gland. Thorax. 24, 729-36.

Murthy, K. S., Zhou, H. & Makhlouf, G. M. (2002). PKA-dependent activation of PDE3A and PDE4 and inhibition of adenylyl cyclase V/VI in smooth muscle. Am J Physiol Cell Physiol. 282, C508-17.

Naren, A. P., Cobb, B., Li, C., Roy, K., Nelson, D., Heda, G. D., Liao, J., Kirk, K. L., Sorscher, E. J., Hanrahan, J. & Clancy, J. P. (2003). A macromolecular complex of beta 2 adrenergic receptor, CFTR, and ezrin/radixin/moesin-binding phosphoprotein 50 is regulated by PKA. Proc Natl Acad Sci U S A. 100, 342-6.

Naren, A. P., Nelson, D. J., Xie, W., Jovov, B., Pevsner, J., Bennett, M. K., Benos, D. J., Quick, M. W. & Kirk, K. L. (1997). Regulation of CFTR chloride channels by syntaxin and Munc18 isoforms. Nature. 390, 302-5.

Naren, A. P., Quick, M. W., Collawn, J. F., Nelson, D. J. & Kirk, K. L. (1998). Syntaxin 1A inhibits CFTR chloride channels by means of domain-specific protein-protein interactions. Proc Natl Acad Sci U S A. 95, 10972-7.

Onuma, H., Osawa, H., Yamada, K., Ogura, T., Tanabe, F., Granner, D. K. & Makino, H. (2002). Identification of the insulin-regulated interaction of phosphodiesterase 3B with 14-3-3 beta protein. Diabetes. 51, 3362-7.

Perry, S. J., Baillie, G. S., Kohout, T. A., McPhee, I., Magiera, M. M., Ang, K. L., Miller, W. E., McLean, A. J., Conti, M., Houslay, M. D. & Lefkowitz, R. J. (2002). Targeting of cyclic AMP degradation to beta 2-adrenergic receptors by beta-arrestins. Science. 298, 834-6.

Peters, K. W., Qi, J., Watkins, S. C. & Frizzell, R. A. (1999). Syntaxin 1A inhibits regulated CFTR trafficking in xenopus oocytes. Am J Physiol. 277, C174-80.

Pilewski, J. M. & Frizzell, R. A. (1999). Role of CFTR in airway disease. Physiol Rev. 79, S215-55.

Ponsioen, B., Zhao, J., Riedl, J., Zwartkruis, F., van der Krogt, G., Zaccolo, M., Moolenaar, W. H., Bos, J. L. & Jalink, K. (2004). Detecting cAMP-induced Epac activation by fluorescence resonance energy transfer: Epac as a novel cAMP indicator. EMBO Rep. 5, 1176-80.

Pozuelo Rubio, M., Campbell, D. G., Morrice, N. A. & Mackintosh, C. (2005). Phosphodiesterase 3A binds to 14-3-3 proteins in response to PMA-induced phosphorylation of Ser428. Biochem J. 392, 163-72.

Puxeddu, E., Uhart, M., Li, C. C., Ahmad, F., Pacheco-Rodriguez, G., Manganiello, V. C., Moss, J. & Vaughan, M. (2009). Interaction of phosphodiesterase 3A with brefeldin A-inhibited guanine nucleotide-exchange proteins BIG1 and BIG2 and effect on ARF1 activity. Proc Natl Acad Sci U S A. 106, 6158-63.

Quinton, P. M. (1983). Chloride impermeability in cystic fibrosis. Nature. 301, 421-2.

Quinton, P. M. (1986). Missing Cl conductance in cystic fibrosis. Am J Physiol. 251, C649-52.

Richter, W. & Conti, M. (2004). The oligomerization state determines regulatory properties and inhibitor sensitivity of type 4 cAMP-specific phosphodiesterases. J Biol Chem. 279, 30338-48.

Riordan, J. R. (2005). Assembly of functional CFTR chloride channels. Annu Rev Physiol. 67, 701-18.

Riordan, J. R. (2008). CFTR function and prospects for therapy. Annu Rev Biochem. 77, 701-26.

Riordan, J. R., Rommens, J. M., Kerem, B., Alon, N., Rozmahel, R., Grzelczak, Z., Zielenski, J., Lok, S., Plavsic, N., Chou, J. L. & et al. (1989). Identification of the cystic fibrosis gene: cloning and characterization of complementary DNA. Science. 245, 1066-73.

Rogers, C. S., Stoltz, D. A., Meyerholz, D. K., Ostedgaard, L. S., Rokhlina, T., Taft, P. J., Rogan, M. P., Pezzulo, A. A., Karp, P. H., Itani, O. A., Kabel, A. C., Wohlford-Lenane, C. L., Davis, G. J., Hanfland, R. A., Smith, T. L., Samuel, M., Wax, D., Murphy, C. N., Rieke, A., Whitworth, K., Uc, A., Starner, T. D., Brogden, K. A., Shilyansky, J., McCray, P. B., Jr., Zabner, J., Prather, R. S. & Welsh, M. J. (2008). Disruption of the CFTR gene produces a model of cystic fibrosis in newborn pigs. Science. 321, 1837-41.

Rogers, D. F. (2003). Pulmonary mucus: Pediatric perspective. Pediatr Pulmonol. 36, 178-88.

Rogers, D. F. (2004). Airway mucus hypersecretion in asthma: an undervalued pathology? Curr Opin Pharmacol. 4, 241-50.

Rowntree, R. K. & Harris, A. (2003). The phenotypic consequences of CFTR mutations. Ann Hum Genet. 67, 471-85.

Salinas, D., Haggie, P. M., Thiagarajah, J. R., Song, Y., Rosbe, K., Finkbeiner, W. E., Nielson, D. W. & Verkman, A. S. (2005). Submucosal gland dysfunction as a primary defect in cystic fibrosis. Faseb J. 19, 431-3.

Samet, J. M. & Cheng, P. W. (1994). The role of airway mucus in pulmonary toxicology. Environ Health Perspect. 102 Suppl 2, 89-103.

Schudt, C., Tenor, H. & Hatzelmann, A. (1995). PDE isoenzymes as targets for anti-asthma drugs. Eur Respir J. 8, 1179-83.

Shakur, Y., Holst, L. S., Landstrom, T. R., Movsesian, M., Degerman, E. & Manganiello, V. (2001). Regulation and function of the cyclic nucleotide phosphodiesterase (PDE3) gene family. Prog Nucleic Acid Res Mol Biol. 66, 241-77.

Sheppard, D. N. & Welsh, M. J. (1999). Structure and function of the CFTR chloride channel. Physiol Rev. 79, S23-45.

Shin, D. D., Brandimarte, F., De Luca, L., Sabbah, H. N., Fonarow, G. C., Filippatos, G., Komajda, M. & Gheorghiade, M. (2007). Review of current and investigational pharmacologic agents for acute heart failure syndromes. Am J Cardiol. 99, 4A-23A.

Short, D. B., Trotter, K. W., Reczek, D., Kreda, S. M., Bretscher, A., Boucher, R. C., Stutts, M. J. & Milgram, S. L. (1998). An apical PDZ protein anchors the cystic fibrosis transmembrane conductance regulator to the cytoskeleton. J Biol Chem. 273, 19797-801.

Sun, F., Hug, M. J., Lewarchik, C. M., Yun, C. H., Bradbury, N. A. & Frizzell, R. A. (2000). E3KARP mediates the association of ezrin and protein kinase A with the cystic fibrosis transmembrane conductance regulator in airway cells. J Biol Chem. 275, 29539-46.

Tasken, K. A., Collas, P., Kemmner, W. A., Witczak, O., Conti, M. & Tasken, K. (2001). Phosphodiesterase 4D and protein kinase a type II constitute a signaling unit in the centrosomal area. J Biol Chem. 276, 21999-2002.

Thompson, P. E., Manganiello, V. & Degerman, E. (2007). Re-discovering PDE3 inhibitors--new opportunities for a long neglected target. Curr Top Med Chem. 7, 421-36.

Thompson, W. J., Terasaki, W. L., Epstein, P. M. & Strada, S. J. (1979). Assay of cyclic nucleotide phosphodiesterase and resolution of multiple molecular forms of the enzyme. Adv Cyclic Nucleotide Res. 10, 69-92.

Torphy, T. J. (1998). Phosphodiesterase isozymes: molecular targets for novel antiasthma agents. Am J Respir Crit Care Med. 157, 351-70.

Trout, L., King, M., Feng, W., Inglis, S. K. & Ballard, S. T. (1998). Inhibition of airway liquid secretion and its effect on the physical properties of airway mucus. Am J Physiol. 274, L258-63.

Ullman, E. F., Kirakossian, H., Switchenko, A. C., Ishkanian, J., Ericson, M., Wartchow, C. A., Pirio, M., Pease, J., Irvin, B. R., Singh, S., Singh, R., Patel, R., Dafforn, A., Davalian, D., Skold, C., Kurn, N. & Wagner, D. B. (1996). Luminescent oxygen channeling assay (LOCI): sensitive, broadly applicable homogeneous immunoassay method. Clin Chem. 42, 1518-26.

Wang, S., Yue, H., Derin, R. B., Guggino, W. B. & Li, M. (2000). Accessory protein facilitated CFTR-CFTR interaction, a molecular mechanism to potentiate the chloride channel activity. Cell. 103, 169-79.

Wine, J. J. & Joo, N. S. (2004). Submucosal glands and airway defense. Proc Am Thorac Soc. 1, 47-53.

Wright, L. C., Seybold, J., Robichaud, A., Adcock, I. M. & Barnes, P. J. (1998). Phosphodiesterase expression in human epithelial cells. Am J Physiol. 275, L694-700.

Wu, P. & Wang, P. (2004). Per-Arnt-Sim domain-dependent association of cAMP-phosphodiesterase 8A1 with IkappaB proteins. Proc Natl Acad Sci U S A. 101, 17634-9.

Yoo, D., Flagg, T. P., Olsen, O., Raghuram, V., Foskett, J. K. & Welling, P. A. (2004). Assembly and trafficking of a multiprotein ROMK (Kir 1.1) channel complex by PDZ interactions. J Biol Chem. 279, 6863-73.

Zaccolo, M. (2006). Phosphodiesterases and compartmentalized cAMP signalling in the heart. Eur J Cell Biol. 85, 693-7.

Zielenski, J. (2000). Genotype and phenotype in cystic fibrosis. Respiration. 67, 117-33.

Zielenski, J. & Tsui, L. C. (1995). Cystic fibrosis: genotypic and phenotypic variations. Annu Rev Genet. 29, 777-807.

Zuelzer, W. W. & Newton, W. A., Jr. (1949). The pathogenesis of fibrocystic disease of the pancreas; a study of 36 cases with special reference to the pulmonary lesions. Pediatrics. 4, 53-69.

VITA

Himabindu Penmatsa was born on February 18, 1977 in India. She received her Bachelor of Science in biochemistry, botany and chemistry in 1997 and Master of Science in biotechnology in 1999 from Andhra University, India. She worked as a lecturer from 1999-2002 and then completed diploma course in bioinformatics in 2002 from Indian Institute of Chemical Technology. She later worked as a project trainee in bioinformatics from 2003-2004. In August 2005 she joined the IPBS program. She received a pre-doctoral fellowship from American Heart Association for 2008-2010 and J. Paul. Quigley award for 2008. Bindu will receive her Doctor of Philosophy degree from The University of Tennessee Health Science Center in December 2009.